The Bulletin of Nagasaki Institute of Applied Science

Analysis on Aerodynamic Characteristics of WIG

— Proposal of New Green's Function considering Water Wave Generation caused by Aerial Vortices —

Tsutomu Hori

Volume 65 , No. 2 *15 January 2026*

長崎総合科学大学 紀 要 第 65 巻 第 2 号 (pp. 49－78)

【 数物系科学 】
〈 研究ノート 〉

Analysis on Aerodynamic Characteristics of WIG
― Proposal of New Green's Function considering Water Wave Generation caused by Aerial Vortices ―[*1]

by Tsutomu HORI [*2]

Summary

In this paper, a Green's function considering water wave generation caused by aerial vortices is proposed. The new function is derived in the form that the influence of pressure fluctuations on the water surface is reflected by using the Fourier transform method.

By performing an asymptotic analysis for the Green's function, it is shown that the high-speed flow field due to an aerial vortex can be represented by placing a slightly weaker vortex at the mirror image position under the water surface. As a result, asymptotic wave profiles at the high speed swells up in the neighborhood of WIG.

Furthermore, the lift force and wave-making resistance acting on the WIG are analyzed based on the momentum theorem, and thereby smart calculation formulae are presented for the two forces. Based on the developed theory, specific numerical calculations of aerodynamic forces and water wave profiles are performed for NACA airfoils as an example of thick wings. Thereby a certain amount of knowledge was obtained about the water surface effects of WIG.

Keywords : ***Aerodynamic Characteristics, WIG, New Green's Function, Water Wave Generation, Aerial Vortices, NACA airfoils***

1. Introduction

The research on water surface effects of WIG (Wing In Ground-effect) was initiated in the field of aeronautics by Tomotika and Imai(2) and Tani(3), but the former assumed $F_n = \infty$ and the latter assumed $F_n = 0$ (where, F_n is Froude number), failing to properly account for the deformation of water surface. Subsequently, in the field of naval architecture in Japan, a pioneering research, taking this into account based on the linear wave-making resistance theory, was conducted by Bessho and Ishikawa(4), followed by Masuda and Suzuki(5) and Kataoka, Ando and Nakatake(6) from the perspective of numerical analysis.

[*1] This paper is essentially an English translation of the Reference (1) written by author, with a detailed description of mathematical derivations.

[*2] *Professor Emeritus*, HORI's Laboratory of Ship Waves and Hydrostatic Stability, Nagasaki Institute of Applied Science, Japan

Received : September 22, 2025 《 The Bulletin of Nagasaki Institute of Applied Science, Vol.65, No.2,
Accepted : November 29, 2025 Research Notes in Mathematical and Physical Science 》

Specifically, Bessho-Ishikawa attempted to analyze the flow field in aerial and underwater sides by connecting the linear free surface conditions of both sides on the water surface, and theoretically determined the both flow fields by neglecting the effect of water surface deformation at the aerial side. On the other hand, Masuda-Suzuki and Kataoka *et al.* basically adopted the same water surface conditions as Bessho-Ishikawa, and numerically computed both flow fields by iterative calculations, taking into account the effects of water surface deformation at aerial and underwater sides.

These studies have shown that the aerodynamic characteristics of the flow field around the WIG, taking the water surface effect into account, can be roughly calculated by using a so-called normal mirror image model in which the water surface is replaced by a rigid wall [3]. Nevertheless, the wave-making phenomenon itself of the water surface caused by aerial vortices is still a subject for further investigation from the viewpoint of ship hydrodynamics.

In view of this situation, this paper constructs a Green's function considering the water wave generation caused by aerial vortices in a 2-dimensional problem. The new function is taken into account pressure fluctuations on the water surface, which was neglected by Bessho-Ishikawa, and is formed by using the Fourier transform method. Then we derive an expression for the flow field at high speeds [1] and a simple formula for asymptotic wave profiles. It is shown that the flow field in the aerial side is represented by the vortex Γ in the air and the image one $(1-2\frac{\varepsilon}{1+\varepsilon})\Gamma$ in the water, where ε *i*s the density ratio of air to water. As a result, asymptotic wave profile at the high speed swells up in the neighborhood of WIG.

Furthermore, the lift force and wave-making resistance acting on the WIG are analyzed based on the momentum theorem, and thereby smart calculation formulae are presented for the two forces. For the former of lift force, it is indicated that the Kutta-Joukowski's theorem also holds in the case of WIG. And regarding the latter of wave-making resistance, an explicit formula is derived by detailed considerations, and it can be calculated only from the amplitude of trailing free waves, without the need for tedious integral over the still water surface. Based on the developed theory, specific numerical calculations of aerodynamic forces and water wave profiles are performed for NACA airfoils as an example of thick wings. Thereby a certain amount of knowledge is provided about the water surface effects of WIG.

We believe that some of this information can be used as a basis for future research, so we would like to report all of you smart readers here and ask for your criticism.

2. Construction of Wave-making Green's Functions caused by Aerial Vortices

The flow field around 2-D WIG is represented as a steady lifting surface problem for the aerial side and underwater side, taking into account wave generations at the interface, the water surface [7].

As shown in Fig. 1, WIG of wing chord length c with an angle of attack α is floating on the aerial side in a uniform flow of size U with free surface at a surfacing altitude h from the still water surface to the trailing edge of the wing. For the analysis, a Cartesian coordinate system is used with the origin o on the still water surface, the x-axis in the uniform flow direction, and the z-axis in the vertical upward direction.

The velocity potentials Φ_A and Φ_W of the flow field on the aerial and underwater sides can be written by superposing the disturbed velocity potentials ϕ_A and ϕ_W on those of the uniform flow U, respectively, as follows :

$$\left.\begin{array}{ll} \textit{Aerial Side} & : \ \Phi_A = Ux + \phi_A \quad (\textit{for } z \geq \zeta) \\ \textit{Underwater Side} & : \ \Phi_W = Ux + \phi_W \quad (\textit{for } z < \zeta) \end{array}\right\} \cdots\cdots\cdots\cdots\cdots\cdots\cdots\cdots\cdots\cdots (1)$$

In this chapter, we will derive the surface conditions and construct the wave-making Green's functions which satisfy them for the above disturbed potentials ϕ_A and ϕ_W, as shown in the following sections.

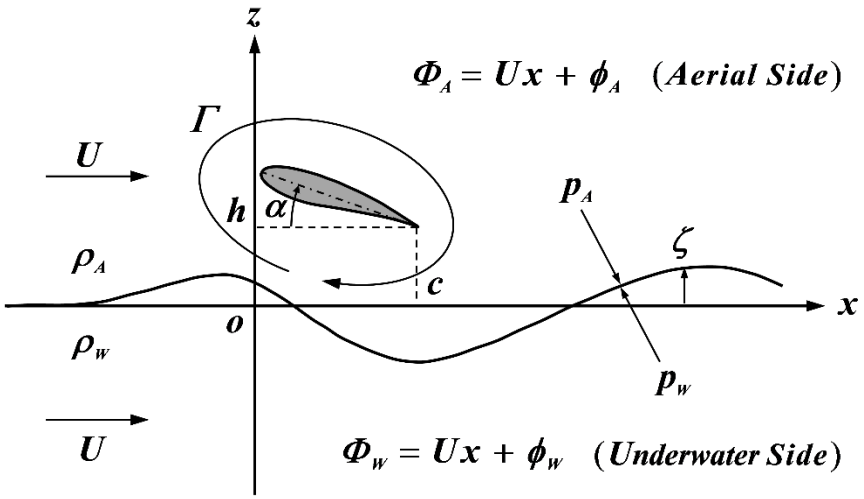

Fig. 1 Coordinate system and definitions of some basic quantities in the problem of WIG.

2.1 Water surface conditions

The pressure condition [D] is imposed that the gauge pressure p_A on the aerial side and the gauge pressure p_W on the underwater side are equal on the water surface at $z = \zeta$, as follows :

$$[D] \quad p_A = p_W = p \ (\neq 0) \quad (on\ z = \zeta) \quad \cdots\cdots\cdots\cdots\cdots\cdots\cdots\cdots\cdots\cdots\cdots\cdots (2)$$

Let us apply the Bernoulli's theorem to the both of the aerial and underwater sides. By considering that the disturbed flow disappears at far upstream $(x \to \infty)$ and linearizing the both equations from the assumption of small wave heights generated by WIG, the condition [D] can be written on the still water surface at $z = \pm 0$, as follows :

$$[D] \quad \left.\begin{array}{ll} \textit{Aerial Side} & : \ \dfrac{\partial \phi_A}{\partial x} + \kappa_0 U\zeta + \mu_A \phi_A = -\dfrac{p}{\rho_A U} \quad (on\ z = +0) \\ \textit{Underwater Side} & : \ \dfrac{\partial \phi_W}{\partial x} + \kappa_0 U\zeta + \mu_W \phi_W = -\dfrac{p}{\rho_W U} \left(= -\varepsilon \dfrac{p}{\rho_A U}\right) \quad (on\ z = -0) \end{array}\right\} \cdots\cdots\cdots (3)$$

Here, unlike the usual problem of water waves caused by underwater disturbances, we cannot set that $p = 0$, *i.e.*, p on the right-hand side is equal to atmospheric pressure.

In the above equation, ε is parameter representing the density ratio of air to water and κ_0 is wave number, each of two are defined as follows :

$$\left.\begin{aligned} \varepsilon &= \frac{\rho_A}{\rho_W}\ (=0.001275 \approx \frac{1}{784}\ \ at\ 4^\circ\mathrm{C}) \\ \kappa_0 &= \frac{g}{U^2} \end{aligned}\right\} \quad \cdots\cdots(4)$$

In addition, μ_A and μ_W in Eq. (3) are Rayleigh's virtual friction coefficients for air and water respectively, and both are set to $\mu_A \to 0$ and $\mu_W \to 0$ after the analysis. And, g is the gravitational acceleration.

On the other hand, the kinematic condition [K], which imposes that the flow moves along the wave surface, can also be written by linearizing in the same way as the pressure conditions [D] in Eq. (3), as follows :

$$[K] \quad \left.\begin{aligned} &Aerial\ Side \quad : \quad \frac{\partial \phi_A}{\partial z} = U\frac{\partial \zeta}{\partial x} \quad (on\ z=+0) \\ &Underwater\ Side \quad : \quad \frac{\partial \phi_W}{\partial z} = U\frac{\partial \zeta}{\partial x} \quad (on\ z=-0) \end{aligned}\right\} \quad \cdots\cdots(5)$$

Here, let us eliminate the wave height ζ by differentiating Eq. (3) with x and substituting Eq. (5) into it. Then if we connect the pressure conditions [D] on the aerial and underwater sides by equating the pressure gradient $\frac{\partial p}{\partial x}$ at $z=+0$ and $z=-0$, the following water surface condition [F] can be obtained :

$$[F] \quad \frac{\partial^2 \phi_A}{\partial x^2} + \kappa_0 \frac{\partial \phi_A}{\partial z} + \mu_A \frac{\partial \phi_A}{\partial x} = \frac{1}{\varepsilon}\left(\frac{\partial^2 \phi_W}{\partial x^2} + \kappa_0 \frac{\partial \phi_W}{\partial z} + \mu_W \frac{\partial \phi_W}{\partial x} \right) \quad (on\ z=0) \quad \cdots\cdots(6)$$

By equating the wave slope $\frac{\partial \zeta}{\partial x}$ in the upper and lower two equations of Eq. (5), the kinematic condition [K] can be rewritten as :

$$[K] \quad \frac{\partial \phi_A}{\partial z} = \frac{\partial \phi_W}{\partial z} \quad (on\ z=0) \quad \cdots\cdots(7)$$

In the next section, we will solve for both disturbed potentials ϕ_A and ϕ_W by coupling Eqs. (6) and (7) above.

2.2 Construction of Green's functions

Let us construct a wave-making Green's function for a clockwise two-dimensional vortex of strength $\Gamma = 2\pi$ at a point (ξ, h) in the air, as shown in Fig. 2. The Green's functions for the aerial and underwater sides are denoted by G'_A and G'_W respectively, and are constructed in the following form :

$$\left.\begin{aligned} &Aerial\ Side \quad : \quad G_A = -\theta + G'_A \quad (for\ z \geq 0) \\ &Underwater\ Side \quad : \quad G_W = G'_W \quad (for\ z \leq 0) \end{aligned}\right\} \quad \cdots\cdots(8)$$

Here, G'_A and G'_W on the right-hand side represent the regular parts of G_A and G_W, respectively.

Then, the disturbed velocity potentials ϕ_A and ϕ_W, corresponding to G'_A and G'_W, can be expressed in the form of boundary integrals along the wing surface ℓ_H respectively, by denoting the distribution density of bound vortices by $\gamma(\xi,h)$, as follows :

$$\left.\begin{aligned}\phi_A &= \frac{1}{2\pi}\int_{\ell_H}\gamma(\xi,h)\,G_A(x,z;\xi,h)\,d\ell_H \\ \phi_W &= \frac{1}{2\pi}\int_{\ell_H}\gamma(\xi,h)\,G_W(x,z;\xi,h)\,d\ell_H\end{aligned}\right\} \quad \cdots\cdots(9)$$

The Green's functions G'_A and G'_W can be determined so as to satisfy the free surface conditions [F] and [K] shown in Eqs. (6) and (7) in the previous section, by using the Fourier transform method[7]. The procedure is described below.

The formal Fourier integral notation of the principal solution $-\theta$, which represents an aerial vortex, for the region $z-h<0$ including the water surface, has the following form :

$$-\theta = -\tan^{-1}\left(\frac{z-h}{x-\xi}\right) = -\,\mathrm{Im}\left[\int_0^\infty e^{k(z-h)+ik(x-\xi)}\,\frac{dk}{k}\right] \quad (for\ z-h<0) \quad \cdots\cdots(10)$$

Here, Im[···] means taking the imaginary part inside the brackets.

Corresponding to the above expression, the regular part of the Green's function G'_A and G'_W are written in the form of Fourier transform of the undetermined kernel functions $\Psi_A(k)$ and $\Psi_W(k)$ respectively, as follows :

$$\left.\begin{aligned}&Aerial\ Side \quad : \quad G'_A = \mathrm{Im}\left[\int_0^\infty \Psi_A(k)\,e^{-kz+ikx}dk\right] \quad (for\ z\ge 0) \\ &Underwater\ Side \quad : \quad G'_W = \mathrm{Im}\left[\int_0^\infty \Psi_W(k)\,e^{kz+ikx}dk\right] \quad (for\ z\le 0)\end{aligned}\right\} \quad \cdots\cdots(11)$$

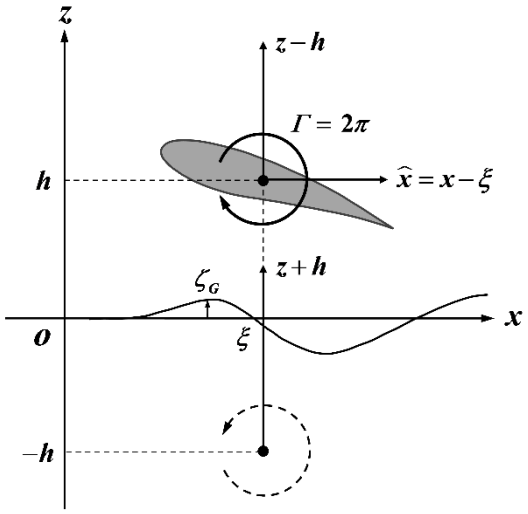

Fig. 2 Coordinate system of Green's function for an aerial vortex.

Hereafter, all Green's functions in complex notation will take their imaginary part and be noted by omitting $\mathrm{Im}[\cdots]$. Here, each of the above integrands is formed so as to satisfy the following z-directional asymptotic behaviors, in which the disturbed flow vanishes at infinite altitude and infinite depth.

$$\left.\begin{array}{ll} \textit{Aerial Side} & : \ G'_A \underset{z\to\infty}{\sim} 0 \\ \textit{Underwater Side} & : \ G'_W \underset{z\to-\infty}{\sim} 0 \end{array}\right\} \quad \cdots\cdots(12)$$

Now, the unknown functions $\Psi_A(k)$ and $\Psi_W(k)$ can be determined so that the Green's functions G'_A and G'_W satisfy the following equations on the still water surface $z=0$ as the free surface conditions in Eqs. (6) and (7).

$$\left.\begin{array}{ll} [F] & \left(\dfrac{\partial^2}{\partial x^2}+\kappa_0\dfrac{\partial}{\partial z}+\mu_A\dfrac{\partial}{\partial x}\right)\left(-\theta+G'_A\right)=\dfrac{1}{\varepsilon}\left(\dfrac{\partial^2}{\partial x^2}+\kappa_0\dfrac{\partial}{\partial z}+\mu_W\dfrac{\partial}{\partial x}\right)G'_W \quad (on\ z=0) \\ [K] & \dfrac{\partial}{\partial z}\left(-\theta+G'_A\right)=\dfrac{\partial}{\partial z}G'_W \quad (on\ z=0) \end{array}\right\} \quad \cdots\cdots\cdots(13)$$

Therefore, by substituting $-\theta$, G'_A and G'_W of Eqs. (10) and (11) into the conditions [F] and [K] of Eq. (13) above and calculating them, the relations between $\Psi_A(k)$ and $\Psi_W(k)$ are obtained as follows :

$$\left.\begin{array}{ll} [F] & \left(k-\kappa_0-i\mu_A\right)e^{-kh-ik\xi}-\left(k+\kappa_0-i\mu_A\right)k\Psi_A(k)=-\dfrac{1}{\varepsilon}\left(k-\kappa_0-i\mu_W\right)k\Psi_W(k) \\ [K] & -\left(e^{-kh-ik\xi}+k\Psi_A(k)\right)=k\Psi_W(k) \end{array}\right\} \quad \cdots\cdots\cdots(14)$$

Then, the above simultaneous equations can be easily solved for $\Psi_A(k)$ and $\Psi_W(k)$ respectively, by putting μ_A and μ_W in the numerator to zero. Accordingly, $\Psi_A(k)$ on the aerial side and $\Psi_W(k)$ on the underwater side are determined as follows :

$$\left.\begin{array}{l} \Psi_A(k)=-(1-2\varepsilon^*)\cdot\dfrac{k-\kappa_0}{k\left(k-\kappa_0^*-i\mu_W^*\right)}\cdot e^{-kh-ik\xi}=\left(-\dfrac{1}{k}+\dfrac{2\varepsilon^*}{k-\kappa_0^*-i\mu_W^*}\right)\cdot e^{-kh-ik\xi} \\ \Psi_W(k)=-\dfrac{2\varepsilon^*}{k-\kappa_0^*-i\mu_W^*}\cdot e^{-kh-ik\xi} \end{array}\right\} \quad \cdots\cdots\cdots(15)$$

The above $\varepsilon^*, \kappa_0^*$ and μ_W^* are modified quantities of the original ε, κ_0 and μ_W by using the air-to-water density ratio ε in Eq. (4), and are defined as follows :

$$\left.\begin{array}{l} \varepsilon^*\equiv\dfrac{\varepsilon}{1+\varepsilon}\ , \quad \mu_W^*\equiv\dfrac{\mu_W+\varepsilon\mu_A}{1+\varepsilon} \\ \kappa_0^*\equiv\dfrac{1-\varepsilon}{1+\varepsilon}\cdot\kappa_0=(1-2\varepsilon^*)\,\kappa_0 \end{array}\right\} \quad \cdots\cdots(16)$$

Since the kernel functions $\Psi_A(k)$ and $\Psi_W(k)$ have been determined in this way, the Green functions G'_A and G'_W are expressed by substituting Eq. (15) into Eq. (11), as shown below.

The Green's function G'_A for the aerial side can be obtained in the following form :

$$G'_A = -\mathrm{Im}\left[\int_0^\infty e^{-k(z+h)+ik(x-\xi)}\frac{dk}{k}\right]_{for\ z+h>0} + 2\varepsilon^*\,\mathrm{Im}\left[\int_0^\infty \frac{1}{k-\kappa_0^*-i\mu_W^*}e^{-k(z+h)+ik(x-\xi)}dk\right]$$

$$= \tan^{-1}\left(\frac{z+h}{x-\xi}\right) + 2\varepsilon^*\,\mathrm{Im}\left[\int_0^\infty \frac{1}{k-\kappa_0^*-i\mu_W^*}e^{-k(z+h)+ik(x-\xi)}dk\right]$$

$$\equiv \theta' + \tilde{G}'_A \quad \cdots\cdots(17)$$

Here, the 1st term represents the counterclockwise vortex θ' at the mirror position $(\xi,-h)$, for the aerial region $z+h>0$ including the water surface. The 2nd term, denoted by $\tilde{G}'_A$, represents the wave generation, and is written as follows :

$$\tilde{G}'_A = 2\varepsilon^*\,\mathrm{Im}\left[\int_0^\infty \frac{1}{k-\kappa_0^*-i\mu_W^*}e^{-k(z+h)+ik(x-\xi)}dk\right] \quad \cdots\cdots(18)$$

Then, the total Green's function G_A in Eq. (8) can be written by the result of Eq. (17), as follows :

$$G_A = -\theta + G'_A = -\theta + (\theta' + \tilde{G}'_A)$$
$$= (-\theta + \theta') + \tilde{G}'_A \equiv G_\Gamma + \tilde{G}'_A \quad \cdots\cdots(19)$$

Here, the 1st and 2nd terms in the 2nd line represent the velocity potential of the double model flow and it is denoted by G_Γ.

On the other hand, the Green's function G'_W for the underwater side is obtained in the following form, and shows the similar characteristics to the wave-making term $\tilde{G}'_A$ for the aerial side in Eq. (18).

$$G'_W\ (=G_W) = -2\varepsilon^*\,\mathrm{Im}\left[\int_0^\infty \frac{1}{k-\kappa_0^*-i\mu_W^*}e^{k(z-h)+ik(x-\xi)}dk\right] \quad \cdots\cdots(20)$$

3. Expression of Wave Height ζ

The wave height ζ can be obtained by equating the pressure p and eliminating it in the pressure condition [D] on the aerial and underwater sides in Eq. (3), as follows :

$$\zeta = -\frac{1}{\kappa_0 U(1-\varepsilon)}\cdot\left(\frac{\partial\phi_W}{\partial x} - \varepsilon\frac{\partial\phi_A}{\partial x}\right)\Bigg]_{z=0} \quad \cdots\cdots(21)$$

Here, in the above calculation process, the virtual friction coefficients μ_A and μ_W are set to zero in Eq. (3).

Also, using Eqs. (8) and (17) for G_A and G_W corresponding to ϕ_A and ϕ_W, the wave height ζ_G is written in the level of Green's function, as follows :

$$\zeta_G = -\frac{1}{\kappa_0 U(1-\varepsilon)} \cdot \left[\frac{\partial}{\partial x} G'_W - \varepsilon \left\{ \frac{\partial}{\partial x}(-\theta + \theta') + \frac{\partial}{\partial x} \tilde{G}'_A \right\} \right]_{z=0} \quad \cdots\cdots (22)$$

Here, by differentiating Eqs. (20) and (18) with x, the following relation holds at $z = 0$ on the still water surface.

$$\left. \frac{\partial G'_W}{\partial x} \right]_{z=0} = -\left. \frac{\partial \tilde{G}'_A}{\partial x} \right]_{z=0} \quad \cdots\cdots (23)$$

By using the above relation and eliminating the underwater Green's function G'_W, the wave height ζ_G in Eq. (22) can be expressed by $\varepsilon^*, \kappa_0^*$ in Eq. (16), as follows :

$$\begin{aligned} \zeta_G &= \frac{1}{\kappa_0 U(1-\varepsilon)} \cdot \left[(1+\varepsilon) \frac{\partial}{\partial x} \tilde{G}'_A - \varepsilon \frac{\partial}{\partial x}(-\theta + \theta') \right]_{z=0} \\ &= \frac{1}{\kappa_0^* U} \cdot \left[\frac{\partial}{\partial x} \tilde{G}'_A + \varepsilon^* \frac{\partial}{\partial x}(-\theta + \theta') \right]_{z=0} = \frac{1}{\kappa_0^* U} \cdot \left\{ \left. \frac{\partial \tilde{G}'_A}{\partial x} \right]_{z=0} - \varepsilon^* \frac{2h}{(x-\xi)^2 + h^2} \right\} \end{aligned} \quad \cdots\cdots (24)$$

Then, by differentiating Eq. (18) with x and substituting it into $\tilde{G}'_A$ above, the following expression is obtained :

$$\begin{aligned} \zeta_G &= \frac{1}{\kappa_0^* U} \cdot \left\{ 2\varepsilon^* \,\mathrm{Im}\left[i \int_0^\infty \frac{k\, e^{-kh+ik\hat{x}}}{k - \kappa_0^* - i\mu_W^*} dk \right] - \frac{2\varepsilon^* h}{\hat{x}^2 + h^2} \right\} \\ &= \frac{2\varepsilon^*}{\kappa_0^* U} \cdot \left\{ \mathrm{Im}\left[i \int_0^\infty e^{-kh+ik\hat{x}} dk + i\kappa_0^* \int_0^\infty \frac{e^{-kh+ik\hat{x}}}{k - \kappa_0^* - i\mu_W^*} dk \right] - \frac{h}{\hat{x}^2 + h^2} \right\} \\ &= \frac{2\varepsilon^*}{\kappa_0^* U} \cdot \left\{ -\frac{\partial}{\partial \hat{x}} \tan^{-1}\left(\frac{h}{\hat{x}} \right) + \mathrm{Re}\left[\kappa_0^* \int_0^\infty \frac{e^{-kh+ik\hat{x}}}{k - \kappa_0^* - i\mu_W^*} dk \right] - \frac{h}{\hat{x}^2 + h^2} \right\} \\ &= \frac{2\varepsilon^*}{U} \cdot \mathrm{Re}\left[\int_0^\infty \frac{e^{-kh+ik\hat{x}}}{k - \kappa_0^* - i\mu_W^*} dk \right] \end{aligned} \quad \cdots\cdots (25)$$

Here, the above equation is the result of the cancellation of the 1st and 3rdd terms in braces $\{...\}$. Re[...] is meant to take the real part for complex notation. Then, $\hat{x}$ is the x-coordinate measured from $x = \xi$, and is defined by :

$$\hat{x} \equiv x - \xi \quad \cdots\cdots (26)$$

Now, let us consider the semi-infinite integral with respect to k in Eq. (25), by extending it onto the Gaussian plane $k + im$. Depending on whether $\hat{x}$ is positive or negative, we apply the residue theorem and transfer the integral on the real axis k to the imaginary axis m, then set $\mu_W^* \to 0$. By doing so, the following meaningful result is obtained :

$$\int_0^\infty \frac{e^{-kh+ik\hat{x}}}{k-\kappa_0^*-i\mu_W^*}\,dk = \begin{cases} \displaystyle\int_0^\infty \frac{e^{-m|\hat{x}|-imh}}{m+i\kappa_0^*}\,dm + 2\pi i\, e^{-\kappa_0^* h+i\kappa_0^*\hat{x}} & (for\ \hat{x}\geq 0) \\ \displaystyle\int_0^\infty \frac{e^{-m|\hat{x}|+imh}}{m-i\kappa_0^*}\,dm = \overline{\int_0^\infty \frac{e^{-m|\hat{x}|-imh}}{m+i\kappa_0^*}\,dm} & (for\ \hat{x}<0) \end{cases}$$

$$= \mathrm{Re}\left[\int_0^\infty \frac{e^{-m|\hat{x}|-imh}}{m+i\kappa_0^*}\,dm\right] + i\,\mathrm{sgn}\,\hat{x}\cdot\mathrm{Im}\left[\int_0^\infty \frac{e^{-m|\hat{x}|-imh}}{m+i\kappa_0^*}\,dm\right] + \pi i\,(1+\mathrm{sgn}\,\hat{x})\,e^{-\kappa_0^* h+i\kappa_0^*|\hat{x}|} \quad \cdots\cdots\cdots\cdots (27)$$

Here, $\overline{(...)}$ means taking the complex conjugate. $\mathrm{sgn}\,\hat{x}$ is signum function and takes +1 and -1 depending on the positive and negative values of $\hat{x}$.

Thus, taking the real part of the above result, the 2nd term becomes unnecessary, and ζ_G in Eq. (25) is expressed as follows :

$$\zeta_G = \frac{2\varepsilon^*}{U}\cdot\mathrm{Re}\left[\int_0^\infty \frac{e^{-m(|\hat{x}|+ih)}}{m+i\kappa_0^*}\,dm + \pi i\,(1+\mathrm{sgn}\,\hat{x})\,e^{-\kappa_0^* h+i\kappa_0^*|\hat{x}|}\right] \quad \cdots\cdots\cdots\cdots\cdots\cdots\cdots\cdots (28)$$

Furthermore, the integral in the above equation is performed by substituting the real variable m with the following complex variable η :

$$\eta = (m+i\kappa_0^*)\cdot(|\hat{x}|+ih) \quad \cdots\cdots\cdots\cdots\cdots\cdots\cdots\cdots\cdots\cdots\cdots\cdots\cdots\cdots\cdots\cdots\cdots\cdots (29)$$

Accordingly, the integral with m can be rewritten to the following integral with η, and it can be expressed as an integral exponential function Ei in the complex plane.

$$\int_0^\infty \frac{e^{-m(|\hat{x}|+ih)}}{m+i\kappa_0^*}\,dm = e^{i\kappa_0^*(|\hat{x}|+ih)}\int_0^\infty \frac{e^{-(m+i\kappa_0^*)\cdot(|\hat{x}|+ih)}}{m+i\kappa_0^*}\,dm$$

$$= e^{i\kappa_0^*(|\hat{x}|+ih)}\int_{\kappa_0^*(|\hat{x}|+ih)}^\infty \frac{e^{-\eta}}{\eta}\,d\eta = -e^{-i\kappa_0^*(|\hat{x}|+ih)}\,\mathrm{Ei}\left(-i\kappa_0^*(|\hat{x}|+ih)\right) \quad \cdots\cdots\cdots (30)$$

By using this result into Eq. (28), the wave height ζ_G can be expressed as follows :

$$\zeta_G = -\frac{2\varepsilon^*}{U}e^{-\kappa_0^* h}\cdot\left\{\mathrm{Re}\left[\mathrm{Ei}\left(-i\kappa_0^*(\hat{x}+ih)\right)e^{i\kappa_0^*|\hat{x}|}\right] + \pi\,(1+\mathrm{sgn}\,\hat{x})\,\sin\kappa_0^*|\hat{x}|\right\} \quad \cdots\cdots\cdots\cdots\cdots (31)$$

Here, $\mathrm{Ei}\left(-i\kappa_0^*(\hat{x}+ih)\right)$ is can be calculated by the following Taylor expansion form [8],[9] :

$$\mathrm{Ei}\left(-i\kappa_0^*(|\hat{x}|+ih)\right) = -\int_{i\kappa_0^*(|\hat{x}|+ih)}^\infty \frac{e^{-\eta}}{\eta}\,d\eta$$

$$= \gamma_0 + \log_e i\kappa_0^*(|\hat{x}|+ih) + \sum_{n=1}^\infty \frac{\left\{-i\kappa_0^*(|\hat{x}|+ih)\right\}^n}{n\cdot n!} \equiv E_C + i\,E_S \quad \cdots\cdots\cdots\cdots (32)$$

Then, Ei is decomposed into the real part E_C and the imaginary part E_S, and both parts are written respectively, as follows :

$$\left.\begin{aligned} E_C &= \gamma_0 + \log_e \kappa_0^* R + \sum_{n=1}^{\infty} \frac{(\kappa_0^* R)^n}{n \cdot n!} \cdot \cos\left\{ n\left(\Theta - \frac{\pi}{2} \right) \right\} \\ E_S &= \frac{\pi}{2} + \Theta + \sum_{n=1}^{\infty} \frac{(\kappa_0^* R)^n}{n \cdot n!} \cdot \sin\left\{ n\left(\Theta - \frac{\pi}{2} \right) \right\} \end{aligned}\right\} \quad \cdots\cdots(33)$$

Here, R, Θ and γ_0 above are defined by :

$$\left.\begin{aligned} &\left|\hat{x}\right| + ih = R e^{i\Theta} \\ &\quad where,\ R = \sqrt{\left|\hat{x}\right|^2 + h^2},\ \ \Theta = \tan^{-1} \frac{h}{\left|\hat{x}\right|} \\ &\gamma_0 = 0.57721\cdots\ (Euler's\ Const.) \end{aligned}\right\} \quad \cdots\cdots(34)$$

Therefore, by using E_C and E_S in Eq.(33), the wave height ζ_G in Eq.(31) can ultimately be expressed as follows :

$$\zeta_G = -\frac{2\varepsilon^*}{U} e^{-\kappa_0^* h} \cdot \left\{ E_C \cos \kappa_0^* \left|\hat{x}\right| - E_S \sin \kappa_0^* \left|\hat{x}\right| + \pi (1 + \operatorname{sgn} \hat{x}) \sin \kappa_0^* \left|\hat{x}\right| \right\} \quad \cdots\cdots(35)$$

Now, the integral exponential function Ei decays by the following order as $\kappa_0 R \to \infty$ due to its asymptotic expansion [8],[9].

$$\mathrm{Ei}\left(\kappa_0^* R \mathrm{e}^{i\Theta} \right) \underset{\kappa_0^* R \to \infty}{\sim} O\left(\frac{\mathrm{e}^{-\kappa_0^* R}}{\kappa_0^* R} \right) \quad \cdots\cdots(36)$$

Then, the real and imaginary parts E_C and E_S of the above Ei disappear far upstream and downstream, as follows :

$$\left.\begin{aligned} E_C &\underset{x \to \pm\infty}{\sim} 0 \\ E_S &\underset{x \to \pm\infty}{\sim} 0 \end{aligned}\right\} \quad \cdots\cdots(37)$$

Hence, the 1st and 2nd terms in Eq.(35) represent the local disturbed wave and the 3rd term represents the trailing free wave. Accordingly, the asymptotic wave profile ζ_G at the downstream can be expressed in the level of Green's function as the following simple form :

$$\zeta_G \underset{x \to \infty}{\sim} -\frac{4\pi\varepsilon^*}{U} e^{-\kappa_0^* h} \sin \kappa_0^* \hat{x} \quad \cdots\cdots(38)$$

In this case, the wave height ζ generated by the WIG can be computed by integrating the product of $\gamma(\xi, h)$ and ζ_G due to the expression in Eq.(9), as follows :

$$\zeta = \frac{1}{2\pi} \int_{\ell_H} \gamma(\xi, h)\, \zeta_G(x - \xi, h)\, d\ell_H \quad \cdots\cdots(39)$$

Therefore, the asymptotic behavior of the wave profile ζ due to WIG can be written as follows :

$$\zeta(x) \underset{x \to \infty}{\sim} -Z_\zeta \sin\left(\kappa_0^* x - \delta_\zeta \right) \quad \cdots\cdots(40)$$

Here, Z_ζ is the wave amplitude in the downstream and δ_ζ is the angle of phase delay, and both are constants.

On the other hand, the wave slope $\frac{\partial \zeta_G}{\partial x}$ can be obtained by using $\tilde{G}'_A$ and G'_W in Eqs. (18), (19), (20) instead of ϕ_A and ϕ_W in Eq. (5), as follows :

$$\frac{\partial \zeta_G}{\partial x} = \frac{\partial}{U\partial z}(G_\Gamma + \tilde{G}'_A)\Big]_{z=0} = \frac{\partial}{U\partial z}\tilde{G}'_A\Big]_{z=0} = \frac{\partial}{U\partial z}G'_W\Big]_{z=0}$$
$$= -\frac{2\varepsilon^*}{U}\cdot \mathrm{Im}\left[\int_0^\infty \frac{k}{k-\kappa_0^*-i\mu_W^*}e^{-kh+ik(x-\xi)}dk\right] \quad \cdots\cdots(41)$$

Thus, the wave height ζ_G can also be calculated by integrating the above equation with x as follows, and the result is obtained as same as Eq. (25).

$$\zeta_G = \int_{-\infty}^{x}\frac{\partial \zeta_G}{\partial x}dx = \frac{2\varepsilon^*}{U}\cdot \mathrm{Im}\left[i\int_0^\infty \frac{1}{k-\kappa_0^*-i\mu_W^*}e^{-kh+ik(x-\xi)}dk\right]$$
$$= \frac{2\varepsilon^*}{U}\cdot \mathrm{Re}\left[\int_0^\infty \frac{1}{k-\kappa_0^*-i\mu_W^*}e^{-kh+ik(x-\xi)}dk\right] \quad \cdots\cdots(42)$$

4. Flow Field at Low and High Speeds

In this chapter, we consider the asymptotic behavior of Green's functions G'_A, G'_W and wave height ζ at the range of low and high speeds, and try to extract the characteristics of the flow field [7].

4.1 Asymptotic behavior at low speed limits $\kappa_0 \to \infty$

Let us consider the approximation of the water surface condition at low speeds. For $\kappa_0 \to \infty$ [2], [F] in Eq. (6) becomes as :

$$[F] \quad \frac{\partial \phi_A}{\partial z} = \frac{1}{\varepsilon}\frac{\partial \phi_W}{\partial z} \qquad (on\ z=0) \quad \cdots\cdots(43)$$

By solving the above [F] and [K] in Eq. (7) simultaneously, the following relation is obtained, and it represents the rigid wall condition [3].

$$\frac{\partial \phi_A}{\partial z} = \frac{\partial \phi_W}{\partial z} = 0 \qquad (on\ z=0) \quad \cdots\cdots(44)$$

And, the above condition can be expressed in the level of Green's function by referring Eq. (8), as follows :

$$\frac{\partial}{\partial z}(-\theta + G'_A) = \frac{\partial}{\partial z}G'_W = 0 \qquad (on\ z=0) \quad \cdots\cdots(45)$$

If the Fourier integral form of Eq. (11) is adopted for G_A' and G_W' in Eq. (45), the kernel functions $\Psi_A(k)$ and $\Psi_W(k)$ can be solved as follows, and both results coincide with the case of $\kappa_0 \to \infty$ in Eq. (15).

$$\left.\begin{aligned} \Psi_A(k) &= -\frac{1}{k} e^{-kh-ik\xi} \\ \Psi_W(k) &= 0 \end{aligned}\right\} \quad \cdots\cdots(46)$$

Accordingly, the Green's function G_A' on the aerial side is obtained by substituting Eq. (46) into Eq. (11), as follows :

$$\begin{aligned} G_A' &\underset{\kappa_0^* \to \infty}{\sim} -\int_0^\infty e^{-k(z+h)} \sin k(x-\xi) \frac{dk}{k} \quad (for\ z+h>0) \\ &= \tan^{-1}\left(\frac{z+h}{x-\xi}\right) = \theta' \end{aligned} \quad \cdots\cdots(47)$$

In the low-speed limit, it is found that G_A' represents a counterclockwise mirror-image vortex θ', which is placed at $(\xi, -h)$ in the water and is same strength and opposite direction as the aerial vortex. Then $\tilde{G}_A'$ due to wave generation becomes zero by referring Eq.(17).

On the other hand, by setting $\Psi_W(k) = 0$ in Eq. (11), the Green's function G_W' on the underwater side asymptotically tends to zero, as follows :

$$G_W' \underset{\kappa_0^* \to \infty}{\sim} 0 \quad \cdots\cdots(48)$$

Therefore, the wave height ζ_G is obtained by setting $G_W' = \tilde{G}_A' = 0$ in Eqs. (22) and (24), as follows :

$$\zeta_G \underset{\kappa_0^* \to \infty}{\sim} \frac{\varepsilon}{\kappa_0 U(1-\varepsilon)} \cdot \frac{\partial}{\partial x}(-\theta + \theta') \Big]_{z=0} = -\frac{\varepsilon^*}{\kappa_0^* U} \cdot \frac{2h}{(x-\xi)^2 + h^2} \quad \cdots\cdots(49)$$

This indicates that the wave height ζ_G in the low-speed limit takes a weakly negative value of about $O(\varepsilon^* / \kappa_0^*)$, and the water surface slightly sinks.

4.2 Asymptotic behavior at high speed limits $\kappa_0 \to 0$

In this section, let us consider the approximation of water surface conditions at high speeds. The pressure condition [D] in Eq. (3) is written by equating p on both sides at the limit of $\kappa_0 \to 0$ [(2)], as follows :

$$[D] \quad \frac{\partial \phi_A}{\partial x} = \frac{1}{\varepsilon} \frac{\partial \phi_W}{\partial x} \quad (on\ z=0) \quad \cdots\cdots(50)$$

In this limit, the water surface condition [F] in Eq. (6) becomes the following form of the 1st order derivative of [D] in Eq. (50) with respect to x :

$$[F] \quad \frac{\partial^2 \phi_A}{\partial x^2} = \frac{1}{\varepsilon}\frac{\partial^2 \phi_W}{\partial x^2} \qquad (on\ z=0) \qquad \cdots\cdots (51)$$

Then, the Green function in Eq. (8) should be determined by simultaneously solving the pressure condition [D] in Eq. (50) and the kinematic condition [K] in Eq. (7), in such a way as to satisfy the following equation :

$$\left.\begin{aligned} [D] \quad & \frac{\partial}{\partial x}(-\theta + G_A') = \frac{1}{\varepsilon}\frac{\partial G_W'}{\partial x} \\ [K] \quad & \frac{\partial}{\partial z}(-\theta + G_A') = \frac{\partial G_W'}{\partial x} \end{aligned}\right\} \qquad \cdots\cdots (52)$$

Proceeding by adopting the Fourier integral form of Eq. (11) for G_A' and G_W' respectively, the kernel functions $\Psi_A(k)$ and $\Psi_W(k)$ are obtained as follows, and the results coincide with the case setting $\kappa_0 \to 0$ in Eq. (15).

$$\left.\begin{aligned} \Psi_A(k) &= -(1-2\varepsilon^*)\frac{e^{-kh-ik\xi}}{k} \\ \Psi_W(k) &= -2\varepsilon^* \frac{e^{-kh-ik\xi}}{k} \end{aligned}\right\} \qquad \cdots\cdots (53)$$

Therefore, the Green's function G_A' in the aerial side is obtained as follows :

$$\begin{aligned} G_A' &\underset{\kappa_0^* \to 0}{\sim} -(1-2\varepsilon^*)\int_0^\infty e^{-k(z+h)} \sin k(x-\xi)\frac{dk}{k} \qquad (for\ z+h>0) \\ &= (1-2\varepsilon^*)\tan^{-1}\left(\frac{z+h}{x-\xi}\right) = (1-2\varepsilon^*)\theta' \end{aligned} \qquad \cdots\cdots (54)$$

In the high-speed limit, the G_A' above represents a counterclockwise vortex $(1-2\varepsilon^*)\theta'$ placed at mirror-image position $(\xi, -h)$ in the water. Its vortex strength is slightly $2\varepsilon^*$ weaker than the original aerial vortex.

On the other hand, the Green's function G_W' in the underwater side is obtained as follows, and it can be represented by a weakly clockwise vortex of strength $2\varepsilon^*$ at the same position (ξ, h) as the original aerial vortex.

$$\begin{aligned} G_W' &\underset{\kappa_0^* \to 0}{\sim} -2\varepsilon^* \int_0^\infty e^{k(z-h)} \sin k(x-\xi)\frac{dk}{k} \qquad (for\ z-h<0) \\ &= -2\varepsilon^* \tan^{-1}\left(\frac{z-h}{x-\xi}\right) = -2\varepsilon^* \theta \end{aligned} \qquad \cdots\cdots (55)$$

Thus, the flow field in the high-speed limit can be expressed concisely by both Eqs. (54) and (55) above, without including the wave-making term. :

Now, substituting above G_W' into the kinematic condition [K] in Eq. (5), the wave slope $\frac{\partial \zeta_G}{\partial x}$ can be calculated. By integrating it with respect to x, the wave height ζ_G in the high-speed limit at $\kappa_0^* \to 0$ is obtained, as follows :

$$\zeta_G \underset{\kappa_0^*\to 0}{\sim} \int_{-\infty}^{x} \frac{\partial \zeta_G}{\partial x} dx = \frac{1}{U}\int_{-\infty}^{x} \frac{\partial G_W'}{\partial z}\Bigg]_{z=0} dx = -\frac{2\varepsilon^*}{U}\int_{-\infty}^{x} \frac{\partial}{\partial z}\tan^{-1}\left(\frac{z-h}{x-\xi}\right)\Bigg]_{z=0} dx$$

$$= -\frac{2\varepsilon^*}{U}\int_{-\infty}^{\hat{x}} \frac{\hat{x}}{\hat{x}^2+h^2} d\hat{x} = \frac{2\varepsilon^*}{U}\left[\log_e \sqrt{\hat{x}^2+h^2}\right]_{\hat{x}}^{\infty} \quad \cdots\cdots\cdots\cdots\cdots\cdots\cdots\cdots (56)$$

However, the above expression is not settled in finite values and diverges logarithmically to positive values. Therefore, changing the method, the high-speed asymptotic solution of ζ_G can be obtained by taking the leading term of E_C and E_S at the limit of $\kappa_0^* \to 0$ in the Taylor expansion form of Eq. (33) and by substituting both into Eq. (35), as follows :

$$\zeta_G \underset{\kappa_0^*\to 0}{\sim} -\frac{2\varepsilon^*}{U}\Big[\gamma_0 + \log_e \kappa_0^* R + \kappa_0^*\left\{R\sin\Theta + \left(\frac{\pi}{2} + \pi\,\mathrm{sgn}\,\hat{x} - \Theta\right)|\hat{x}| - h\left(\gamma_0 + \log_e \kappa_0^* R\right)\right\}\Big] + O(\kappa_0^{*2}) \quad \cdots\cdots (57)$$

By calculating the above formula, the wave height ζ_G at $\hat{x} = O(1)$, which is not too far from the vortex, can be estimated approximately. And the asymptotic value at the high-speed of $\kappa_0^* \to 0$ is the order of $-\frac{2\varepsilon^*}{U}\log_e \kappa_0^* R$ (> 0). Here, R, Θ and γ_0 above are defined by Eq. (34). This indicates that the wave height near the clockwise aerial vortex is obtained positively and the wave surface is raised in the high speed range.

5. Lift Force and Wave-making Resistance

Let us apply the momentum theorem to the control surface in the aerial side where $z \geq \zeta$, as shown in Fig. 3. If the unit normal vector pointing inwards to fluid is denoted by $\boldsymbol{n}\,(= n_x \boldsymbol{i} + n_z \boldsymbol{k})$, the velocity vector of flow by $\boldsymbol{q} = (U + u_A)\boldsymbol{i} + w_A \boldsymbol{k}$ and the flow velocity in $\boldsymbol{n}$ - direction by $q_n\,(= \boldsymbol{q} \bullet \boldsymbol{n})$, the following equation is obtained :

$$\int_{\ell_H + \ell_F + \ell_\infty} \left\{ q_n \boldsymbol{q} + \left(\frac{p}{\rho_A} + g z\right)\boldsymbol{n} \right\} d\ell = \boldsymbol{0} \quad \cdots\cdots\cdots\cdots\cdots\cdots\cdots\cdots\cdots\cdots\cdots\cdots (58)$$

Here, we cannot set $p = 0$ on the water surface ℓ_F, *i.e.*, p is equal to atmospheric pressure, unlike the usual problem of water waves caused by underwater disturbances. Taking this into account, the aerodynamic force $\boldsymbol{F}\,(= F_x \boldsymbol{i} + F_z \boldsymbol{k})$ acting on the WIG, surrounding by wing contour ℓ_H, can be calculated by the following boundary integral :

$$\frac{\boldsymbol{F}}{\rho_A} = -\int_{\ell_H} p\,\boldsymbol{n}\, d\ell = g A_H \boldsymbol{k} + \int_{\ell_F + \ell_\infty} \left\{ q_n \boldsymbol{q} - \left(U u_A + \frac{u_A^2 + w_A^2}{2}\right)\boldsymbol{n} \right\} d\ell \quad \cdots\cdots\cdots\cdots\cdots\cdots\cdots (59)$$

In the above integral, the three far boundaries $\ell_D + \ell_T + \ell_U$ are connected and denoted by ℓ_∞.

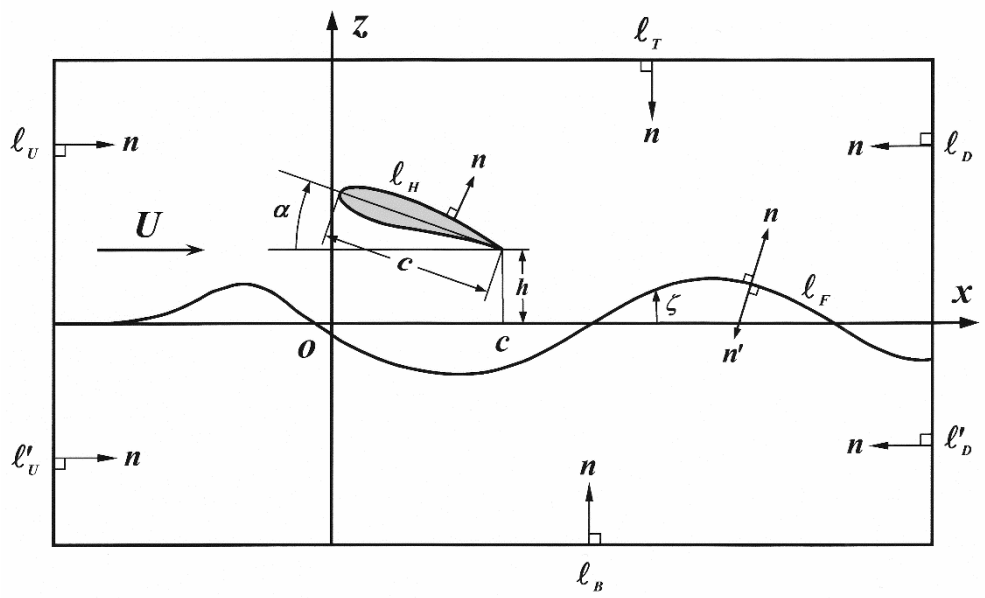

Fig. 3 Control surface of the momentum theorem around WIG.

5.1 Lift force

Let us consider the aerodynamic force F_z in the z-direction. The lift force L can be obtained by excluding the static buoyant force $\rho_A g A_H$ from the z-component of Eq. (59), as follows :

$$\begin{aligned}\frac{L}{\rho_A} &= \frac{F_z}{\rho_A} - g A_H \\ &= \int_{\ell_F+\ell_\infty} \left\{ q_n w_A - \left(U u_A + \frac{u_A^2 + w_A^2}{2} \right) n_z \right\} d\ell \end{aligned} \quad \cdots\cdots(60)$$

Here, A_H is the area of wing cross-section, and q_n and n_z take the following values at the four surrounding boundaries ℓ_F, ℓ_T, ℓ_U, ℓ_D respectively :

$$\left.\begin{array}{ll} \ell_F\ (Free\ Suface\ of\ Water) : & q_n = 0\ ,\ n_z d\ell = dx \\ \ell_T\ (Top\ of\ Ceiling) : & q_n = -w_A\ ,\ n_z = -1 \\ \ell_U\ (Upstream) : & q_n = U + u_A\ ,\ n_z = 0 \\ \ell_D\ (Downstream) : & q_n = -(U + u_A)\ ,\ n_z = 0 \end{array}\right\} \quad \cdots\cdots(61)$$

Accordingly, lift force L in Eq. (60) is written as follows :

$$\begin{aligned}\frac{L}{\rho_A} &= -\int_{\ell_F} \left(U u_A + \frac{u_A^2 + w_A^2}{2} \right) dx + \int_{\ell_T} \left\{ -w_A^2 + \left(U u_A + \frac{u_A^2 + w_A^2}{2} \right) \right\} dx \\ &\quad + \int_{\ell_U} (U + u_A) w_A\, dz - \int_{\ell_D} (U + u_A) w_A\, dz \end{aligned} \quad \cdots\cdots(62)$$

If we neglect the 2nd order terms and extract only the linear terms of the disturbed flow, the above equation can be expressed in counterclockwise circumferential integral for the infinity control surface, as follows :

$$\frac{L}{\rho_A} = -U\int_{-\infty}^{\infty} u_A \Big]_{\substack{\ell_F \\ z=0}} dx - U\int_{0}^{\infty} w_A \Big]_{\substack{\ell_D \\ x=\infty}} dz - U\int_{\infty}^{-\infty} u_A \Big]_{\substack{\ell_T \\ z=\infty}} dx - U\int_{\infty}^{0} w_A \Big]_{\substack{\ell_U \\ x=-\infty}} dz$$

$$= -U\oint_{\ell_F+\ell_D+\ell_T+\ell_U} \left(u_A\,dx + w_A\,dz \right) = -U\oint_{\ell_F+\ell_\infty} \left(u_A\,dx + w_A\,dz \right) \quad \cdots\cdots\cdots\cdots\cdots\cdots (63)$$

The above equation is expressed in terms of velocity potentials, as follows :

$$\frac{L}{\rho_A} = -U\oint_{\ell_F+\ell_\infty} \left(\frac{\partial \phi_A}{\partial x}\,dx + \frac{\partial \phi_A}{\partial z}\,dz \right) = -U\oint_{\ell_F+\ell_\infty} d\phi_A$$

$$= -U\oint_{\ell_F+\ell_\infty} \left(d\phi_\Gamma + d\tilde{\phi}_A \right) = -U\oint_{\ell_F+\ell_\infty} d\phi_\Gamma$$

$$= -U\int_0^{2\pi} \left(-\frac{\Gamma}{2\pi} \right) d\theta = U\Gamma \quad \cdots\cdots\cdots\cdots\cdots\cdots\cdots\cdots\cdots\cdots\cdots\cdots\cdots\cdots\cdots\cdots\cdots\cdots (64)$$

In the above calculation process, $\tilde{\phi}_A$ corresponds to $\tilde{G}'_A$ in Eq. (18) and is regular in the aerial side, so the contour integral value is zero. And ϕ_Γ , corresponding to G_Γ in Eq. (19), is the velocity potential of the double model flow due to the aerial vortex plus the mirror image vortex, so it has a circulation Γ resulting from the contour integral value.

Therefore, the lift force L is obtained in the following form by referring to Eq. (9), and it indicates that the Kutta-Joukowski's theorem holds for the lift of the WIG as well, same as an ordinary wing.

$$L = \rho_A U\Gamma = \rho_A U\oint_{\ell_H} \gamma(\xi, h)\,d\ell_H \quad \cdots\cdots\cdots\cdots\cdots\cdots\cdots\cdots\cdots\cdots\cdots\cdots\cdots\cdots\cdots\cdots\cdots\cdots (65)$$

Then, the lift coefficient C_L is defined by :

$$C_L = \frac{L}{\frac{1}{2}\rho_A U^2 c} \quad \cdots\cdots\cdots\cdots\cdots\cdots\cdots\cdots\cdots\cdots\cdots\cdots\cdots\cdots\cdots\cdots\cdots\cdots\cdots\cdots\cdots\cdots\cdots\cdots (66)$$

5.2 Wave-making resistance

The aerodynamic force F_x in the z-direction can be obtained by taking the x-component of Eq. (59), as follows :

$$\frac{F_x}{\rho_A} = \int_{\ell_F+\ell_\infty} \left\{ q_n\,(U+u_A) - \left(Uu_A + \frac{u_A^2+w_A^2}{2} \right) n_x \right\} d\ell \quad \cdots\cdots\cdots\cdots\cdots\cdots\cdots\cdots\cdots\cdots\cdots\cdots\cdots\cdots (67)$$

The above F_x is the so-called wave-making resistance R_W . Here, q_n and n_x take the following values at the four surrounding boundaries ℓ_F, ℓ_T, ℓ_U, ℓ_D respectively.

$$\left.\begin{array}{ll} \ell_F\,(\,Free\ Suface\ of\ Water\,) & :\ q_n = 0\ ,\ n_x\,d\ell = \dfrac{n_x}{n_z}\cdot n_z\,d\ell = -\dfrac{\partial \zeta}{\partial x}\,dx \\ \ell_T\,(\,Top\ of\ Ceiling\,) & :\ q_n = -w_A\ ,\ n_x = 0 \\ \ell_F\,(\,Upstream\,) & :\ q_n = U + u_A\ ,\ n_x = +1 \\ \ell_F\,(\,Downstream\,) & :\ q_n = -(U+u_A)\ ,\ n_x = -1 \end{array}\right\} \quad \cdots\cdots\cdots\cdots\cdots\cdots (68)$$

Furthermore, R_W in Eq. (67) can be written as follows :

$$\begin{aligned} \frac{R_W}{\rho_A} = & \int_{\ell_F}\left(U u_A + \frac{u_A^2 + w_A^2}{2}\right)\cdot\frac{\partial \zeta}{\partial x}\,dx - \int_{\ell_T} w_A\,(U+u_A)\,dx \\ & + \int_{\ell_U}\left\{\,(U+u_A)^2 - \left(U u_A + \frac{u_A^2 + w_A^2}{2}\right)\right\}dz + \int_{\ell_D}\left\{-(U+u_A)^2 + \left(U u_A + \frac{u_A^2 + w_A^2}{2}\right)\right\}dz \quad \cdots\cdots (69) \end{aligned}$$

Then, with a slight deformation of the 2nd line, we obtain as :

$$\begin{aligned} \frac{R_W}{\rho_A} = & \int_{\ell_F}\left(U u_A + \frac{u_A^2 + w_A^2}{2}\right)\cdot\frac{\partial \zeta}{\partial x}\,dx - \int_{\ell_T} w_A\,(U+u_A)\,dx \\ & + \int_{\ell_U}\left\{U\,(U+u_A) + \frac{u_A^2 - w_A^2}{2}\right\}dz - \int_{\ell_U}\left\{U\,(U+u_A) + \frac{u_A^2 - w_A^2}{2}\right\}dz \quad \cdots\cdots\cdots\cdots\cdots (70) \end{aligned}$$

Here, the following continuous condition of flow holds as :

$$\int_{\ell_U}(U+u_A)\,dz - \int_{\ell_D}(U+u_A)\,dz - \int_{\ell_T} w_A\,dx\ =\ 0 \quad \cdots\cdots\cdots\cdots\cdots\cdots\cdots\cdots\cdots\cdots (71)$$

And, by the kinematic condition [K] of Eq. (5), the wave slope $\dfrac{\partial \zeta}{\partial x}$ is written as :

$$\frac{\partial \zeta}{\partial x} = \frac{w_A}{U} \quad \cdots\cdots\cdots\cdots\cdots\cdots\cdots\cdots\cdots\cdots\cdots\cdots\cdots\cdots\cdots\cdots\cdots\cdots\cdots\cdots (72)$$

Using the above two conditions and deforming Eq.(70), it can be expressed as follows :

$$\frac{R_W}{\rho_A} = \int_{\ell_F}\left(u_A + \frac{u_A^2 + w_A^2}{2U}\right)w_A\,dx - \int_{\ell_T} u_A w_A\,dx + \int_{\ell_U}\frac{u_A^2 - w_A^2}{2}\,dz - \int_{\ell_D}\frac{u_A^2 - w_A^2}{2}\,dz \quad \cdots\cdots\cdots (73)$$

By neglecting the minute quantities over the 3rd order due to the disturbed flow, the above Eq. (73) can be written in the following form, and the values on ℓ_F can be concisely calculated on $z = 0$.

$$\frac{R_W}{\rho_A} = \int_{\ell_F} u_A w_A\,\big]_{z=0}\,dx - \int_{\ell_T} u_A w_A\,dx - \int_{\ell_U}\frac{w_A^2 - u_A^2}{2}\,dz\ +\ \int_{\ell_D}\frac{w_A^2 - u_A^2}{2}\,dz \quad \cdots\cdots\cdots\cdots (74)$$

If the surrounding control surfaces are set to infinite distance, the boundary integrals on ℓ_F and ℓ_D, where the trailing wavy flows $\tilde{u}_W$ and $\tilde{w}_W$ exist, remain only, and those on ℓ_T and ℓ_U disappear.

Therefore, the wave-making resistance R_W can be obtained as follows :

$$\frac{R_W}{\rho_A}=\int_{-\infty}^{\infty}u_A w_A\,\Big]_{z=0}dx+\int_0^{\infty}\frac{\tilde{w}_A^{\,2}-\tilde{u}_A^{\,2}}{2}\Bigg]_{x=\infty}dz \qquad \cdots\cdots(75)$$

This result indicates that R_W cannot be calculated solely from information on the downstream ℓ_D, unlike in the case of normal underwater disturbances, and requires an integral operation over the still water surface $z=0$.

5.2.1 Consideration (A) for the formula of wave-making resistance

In this section, the momentum theorem similar to Eq. (67) is applied to the regular underwater side $\ell_F+\ell'_\infty$ with no disturbance source where $z\le\zeta$, by using $\boldsymbol{q}'=(U+u_W)\boldsymbol{i}+w_W\boldsymbol{k}$, $\boldsymbol{n}'\,(=n'_x\boldsymbol{i}+n'_z\boldsymbol{k})$ and $q'_n\,(=\boldsymbol{q}'\bullet\boldsymbol{n}')$, as shown in Fig. 3. Then the following equation for the z-component is obtained :

$$\int_{\ell_F+\ell'_\infty}\left\{q'_n(U+u_W)-\left(Uu_W+\frac{u_W^2+w_W^2}{2}\right)n'_x\right\}d\ell=0 \qquad \cdots\cdots(76)$$

Here, the quantities on ℓ'_U and ℓ'_D are the same as those in the aerial side of Eq. (68). However, it should be noted that the following values are used on ℓ_F and ℓ_B :

$$\left.\begin{aligned}&\ell_F\,(\textit{Free Suface of Water}) \;:\; n'_x\,d\ell=\frac{\partial\zeta}{\partial x}dx\\&\ell_B\,(\textit{Bottom of Water}) \;:\; q'_n=w_W\end{aligned}\right\} \qquad \cdots\cdots(77)$$

Therefore, by deforming in the same way as Eq. (70), the above Eq. (76) can be written as follows :

$$\begin{aligned}&-\int_{\ell_F}\left(Uu_W+\frac{u_W^2+w_W^2}{2}\right)\cdot\frac{\partial\zeta}{\partial x}dx+\int_{\ell_B}w_W(U+u_W)dx\\&\quad+\int_{\ell'_U}\left\{U(U+u_W)+\frac{u_W^2-w_W^2}{2}\right\}dz-\int_{\ell'_U}\left\{U(U+u_W)+\frac{u_W^2-w_W^2}{2}\right\}dz=0\end{aligned} \qquad \cdots\cdots(78)$$

Here, the continuous condition of flow similar to Eq. (71), and the same kinematic condition [K] as Eq. (72) hold for the underwater side, as follows :

$$\left.\begin{aligned}&\int_{\ell_U}(U+u_W)\,dz-\int_{\ell_D}(U+u_W)\,dz+\int_{\ell_B}w_W\,dx\;=\;0\\&\frac{\partial\zeta}{\partial x}=\frac{w_W}{U}\end{aligned}\right\} \qquad \cdots\cdots(79)$$

By using the above conditions, Eq.(78) can be deformed as follows :

$$-\int_{\ell_F}\left(u_W+\frac{u_W^2+w_W^2}{2U}\right)w_W dx+\int_{\ell_B}u_W w_W dx+\int_{\ell_U}\frac{u_W^2-w_W^2}{2}dz-\int_{\ell_D}\frac{u_W^2-w_W^2}{2}dz=0 \qquad \cdots\cdots(80)$$

Here, as in Eq. (74), if we omit the minute quantities over the 3rd order and approximately replace the water surface ℓ_F with $z=0$, Eq. (80) can be written as follows :

$$-\int_{\ell_F} u_W w_W \Big]_{z=0} dx + \int_{\ell_B} u_W w_W dx - \int_{\ell_U} \frac{w_W^2 - u_W^2}{2} dz + \int_{\ell_D} \frac{w_W^2 - u_W^2}{2} dz = 0 \quad \cdots\cdots\cdots\cdots (81)$$

Furthermore, by setting the control surface to infinite distance similar to Eq. (75), the boundary integrals on ℓ_F and ℓ_D affected by trailing wavy flows $\tilde{u}_W$ and $\tilde{w}_W$ remain only and the following relation can be obtained :

$$\int_{-\infty}^{\infty} u_W w_W \Big]_{z=0} dx = \int_{-\infty}^{0} \frac{\tilde{w}_W{}^2 - \tilde{u}_W{}^2}{2} \Bigg]_{x=\infty} dz \quad \cdots\cdots\cdots\cdots (82)$$

Now, the wavy velocities $\tilde{u}_W$ and $\tilde{w}_W$ at the downstream are related between the aerial and underwater sides, by referring the Green's functions, $\tilde{G}'_A$ in Eq. (18) and G'_W in Eq. (20), as follows :

$$\left.\begin{aligned} \tilde{u}_W(-z) &= -\tilde{u}_A(z) \\ \tilde{w}_W(-z) &= \tilde{w}_A(z) \end{aligned}\right\} \quad \cdots\cdots\cdots\cdots (83)$$

By the above relation, the integral of the 2nd term in Eq. (82) can be written by the velocity components $\tilde{u}_A$ and $\tilde{w}_A$ on the aerial side, as follows :

$$\int_{-\infty}^{0} \frac{\tilde{w}_W{}^2 - \tilde{u}_W{}^2}{2} \Bigg]_{x=\infty} dz = \int_{0}^{\infty} \frac{\tilde{w}_A{}^2 - \tilde{u}_A{}^2}{2} \Bigg]_{x=\infty} dz \quad \cdots\cdots\cdots\cdots (84)$$

Therefore, coupling both Eqs. (82) and (84), the following relation is obtained as :

$$\int_{0}^{\infty} \frac{\tilde{w}_A{}^2 - \tilde{u}_A{}^2}{2} \Bigg]_{x=\infty} dz = \int_{-\infty}^{\infty} u_W w_W \Big]_{z=0} dx \quad \cdots\cdots\cdots\cdots (85)$$

Here, this result indicates that the integral on the downstream control surface in the aerial side can be replaced with the integral on the still water surface in the underwater side.

Adopting the above relation into the 2nd term of Eq. (75), the wave-making resistance R_W can be expressed as the sum of integrals of the product of x-z directional velocity components in both aerial and underwater sides over the still water surface, as follows :

$$\frac{R_W}{\rho_A} = \int_{-\infty}^{\infty} \Big[u_A w_A + u_W w_W \Big]_{z=0} dx \quad \cdots\cdots\cdots\cdots (86)$$

Here, the x-component u_A of the aerial disturbed flow can be written by differentiating Eq. (19) with x, as follows :

$$u_A = u_T + \tilde{u}_A \quad \cdots\cdots\cdots\cdots (87)$$

Then, the wavy component $\tilde{u}_A$ has the following relation on the still water surface $z = 0$, according to Eqs. (18) and (20).

$$\tilde{u}_A = -u_W \quad (on\ z = 0) \quad \cdots\cdots\cdots\cdots (88)$$

Using both Eqs. (87) and (88), the following relation is obtained :

$$u_A + u_W = u_\Gamma \quad (on\ z = 0) \qquad \cdots\cdots(89)$$

Also, the z-component of the disturbed flow has the following relation, according to the water surface condition [K] in Eq. (7).

$$w_A = w_W \quad (on\ z = 0) \qquad \cdots\cdots(90)$$

Hence, the wave-making resistance R_W in Eq. (86) can be rewritten as follows, taking into account Eqs. (89) and (90).

$$\frac{R_W}{\rho_A} = \int_{-\infty}^{\infty} \left(u_A + u_W\right) w_A \Big]_{z=0} dx = \int_{-\infty}^{\infty} u_\Gamma w_A \Big]_{z=0} dx \qquad \cdots\cdots(91)$$

Furthermore, using the wave slope $\dfrac{\partial \zeta}{\partial x}$ in Eq. (72), R_W above can be calculated in the following form :

$$\frac{R_W}{\rho_A} = U \int_{-\infty}^{\infty} \frac{\partial \zeta}{\partial x} \cdot u_\Gamma \Big]_{z=0} dx \qquad \cdots\cdots(92)$$

Here, u_Γ is the aerial vortex flow with the underwater mirror image, and its upstream and downstream flows damp at $O(1/x^2)$ in the far distance. Therefore, the numerical calculation for the above formula is easily performed.

5.2.2 Expression of the wavy disturbed velocity at far downstream

In preparation for the next section, let us consider the expression of the aerial disturbed flow caused by wave generation at far downstream.

The wave height ζ, expressed in the form of the velocity potential in Eq. (21), can be denoted by u_A and u_W, as follows :

$$\zeta = -\frac{1}{\kappa_0 U(1-\varepsilon)} \cdot \left(u_W - \varepsilon u_A \right) \Big]_{z=0} \qquad \cdots\cdots(93)$$

Here, by using the both Eqs. (87) and (88), ζ can be expressed as follows :

$$\begin{aligned} \zeta &= -\frac{1}{\kappa_0 U(1-\varepsilon)} \cdot \left\{ -\tilde{u}_A - \varepsilon (u_\Gamma + \tilde{u}_A) \right\} \Big]_{z=0} \\ &= \frac{1}{\kappa_0 U(1-\varepsilon)} \cdot \left\{ (1+\varepsilon)\, \tilde{u}_A + \varepsilon u_\Gamma \right\} \Big]_{z=0} = \frac{1}{\kappa_0^* U} \cdot \left(\tilde{u}_A + \varepsilon^* u_\Gamma \right) \Big]_{z=0} \end{aligned} \qquad \cdots\cdots(94)$$

The above equation is consistent with Eq. (24) expressed in the level of Green's function. And by solving this for $\tilde{u}_A$ on the still water surface, the following relation is obtained :

$$\tilde{u}_A \Big]_{z=0} = \kappa_0^* U \zeta - \varepsilon^* u_\Gamma \Big]_{z=0} \qquad \cdots\cdots(95)$$

Here, at far downstream, the double model flow u_Γ disappears and the wave height ζ has the form of Eq. (40), so the *x*-directional component $\tilde{u}_A$ of wavy flow on $z=0$ has the simple following form :

$$\tilde{u}_A\big]_{z=0} \underset{x\to\infty}{\sim} \kappa_0^* U\zeta\big]_{x=\infty} = -\kappa_0^* U Z_\zeta \sin\left(\kappa_0^* x - \delta_\zeta\right) \quad \cdots\cdots(96)$$

Thus, the asymptotic form of the wavy disturbed velocity potential $\tilde{\phi}_A$ in the aerial side at the downstream can be expressed by considering the form of $\tilde{G}'_A$ in Eq. (18) for the *z* direction, as follows :

$$\tilde{\phi}_A \underset{x\to\infty}{\sim} U Z_\zeta e^{-\kappa_0^* z} \cos\left(\kappa_0^* x - \delta_\zeta\right) \quad \cdots\cdots(97)$$

Therefore, the wavy velocity components $\tilde{u}_A$ and $\tilde{w}_A$ in the *x* and *z* directions at far downstream are obtained respectively, as follows :

$$\left.\begin{aligned} \tilde{u}_A &= \frac{\partial\tilde{\phi}_A}{\partial x} \underset{x\to\infty}{\sim} -\kappa_0^* U Z_\zeta\, e^{-\kappa_0^* z} \sin\left(\kappa_0^* x - \delta_\zeta\right) \\ \tilde{w}_A &= \frac{\partial\tilde{\phi}_A}{\partial z} \underset{x\to\infty}{\sim} -\kappa_0^* U Z_\zeta\, e^{-\kappa_0^* z} \cos\left(\kappa_0^* x - \delta_\zeta\right) \end{aligned}\right\} \quad \cdots\cdots(98)$$

5.2.3 Consideration (B) for the formula of wave-making resistance

In this section, let us reconsider the wave-making resistance formula, shown in Eq. (75), by using the asymptotic expressions of wavy disturbed velocities in the previous section.

First, the 1st term of Eq. (75) is denoted by Ξ_1, and its integrand can be rewritten by using Eqs. (87), (95) and (72), as follows :

$$\begin{aligned} u_A w_A\big]_{z=0} &= (u_\Gamma + \tilde{u}_A) w_A \\ &= \left\{ u_\Gamma + (\kappa_0^* U\zeta - \varepsilon^* u_\Gamma) \right\} \cdot U \frac{\partial\zeta}{\partial x} \\ &= U(1-\varepsilon^*) \frac{\partial\zeta}{\partial x} u_\Gamma\big]_{z=0} + \frac{1}{2}\kappa_0^* U^2 \frac{\partial}{\partial x}\zeta^2 \end{aligned} \quad \cdots\cdots(99)$$

Accordingly, by integrating the above equation over the still water surface, Ξ_1 can be expressed as follows :

$$\begin{aligned} \Xi_1 &\equiv \int_{-\infty}^{\infty} u_A w_A\big]_{z=0}\, dx \\ &= U(1-\varepsilon^*) \int_{-\infty}^{\infty} \frac{\partial\zeta}{\partial x} u_\Gamma\big]_{z=0} dx + \frac{1}{2}\kappa_0^* U^2 \int_{-\infty}^{\infty} \frac{\partial}{\partial x}\zeta^2 dx \\ &= U(1-\varepsilon^*) \int_{-\infty}^{\infty} \frac{\partial\zeta}{\partial x} u_\Gamma\big]_{z=0} dx + \frac{1}{2}\kappa_0^* U^2 \zeta^2\big]_{x=\infty} \\ &= U(1-\varepsilon^*) \int_{-\infty}^{\infty} \frac{\partial\zeta}{\partial x} u_\Gamma\big]_{z=0} dx + \frac{1}{2\kappa_0^*} \tilde{u}_A{}^2\big]_{\substack{z=0 \\ x=\infty}} \end{aligned} \quad \cdots\cdots(100)$$

Here, the 2nd term is deformed by using the conditions that the wave height ζ is not generated at the upstream $(x=-\infty)$ and is related to $\tilde{u}_A$ as Eq. (96) at the downstream $(x=\infty)$.

Next, let us consider the 2nd term, denoted by Ξ_2, in Eq. (75). Since the wavy flows $\tilde{u}_A$ and $\tilde{w}_A$ at far downstream are expressed by Eq. (98), the integral for the z-direction can be performed analytically and the explicit expression is yielded, as follows :

$$\begin{aligned}\Xi_2 &\equiv \int_0^\infty \frac{\tilde{w}_A{}^2-\tilde{u}_A{}^2}{2}\Big]_{x=\infty} dz \\ &= \frac{1}{2}\left\{\left(-\kappa_0^* U Z_\zeta \cos(\kappa_0^* x-\delta_\zeta)\right)^2-\left(-\kappa_0^* U Z_\zeta \sin(\kappa_0^* x-\delta_\zeta)\right)^2\right\}\int_0^\infty e^{-2\kappa_0^* z}dz \\ &= \frac{1}{4\kappa_0^*}\left\{\tilde{w}_A{}^2\Big]_{\substack{z=0\\x=\infty}}-\tilde{u}_A{}^2\Big]_{\substack{z=0\\x=\infty}}\right\} \qquad \cdots\cdots(101)\end{aligned}$$

Therefore, adding Ξ_1 in Eq. (100) and Ξ_2 in Eq. (101), the wave-making resistance R_W in Eq. (75) is rewritten as follows :

$$\begin{aligned}\frac{R_W}{\rho_A} &= \Xi_1+\Xi_2 \\ &= U(1-\varepsilon^*)\int_{-\infty}^{\infty}\frac{\partial\zeta}{\partial x}u_\Gamma\Big]_{z=0}dx+\frac{1}{4\kappa_0^*}\left\{2\tilde{u}_A{}^2+\left(\tilde{w}_A{}^2-\tilde{u}_A{}^2\right)\right\}\Big]_{\substack{z=0\\x=\infty}} \\ &= U(1-\varepsilon^*)\int_{-\infty}^{\infty}\frac{\partial\zeta}{\partial x}u_\Gamma\Big]_{z=0}dx+\frac{1}{4\kappa_0^*}\left(\tilde{u}_A{}^2+\tilde{w}_A{}^2\right)\Big]_{\substack{z=0\\x=\infty}} \\ &= U(1-\varepsilon^*)\int_{-\infty}^{\infty}\frac{\partial\zeta}{\partial x}u_\Gamma\Big]_{z=0}dx+\frac{\kappa_0^* U^2}{4}Z_\zeta{}^2 \qquad \cdots\cdots(102)\end{aligned}$$

Here, the 2nd term above is expressed in terms of the amplitude Z_ζ of the free wave at downstream, by using Eq. (98).

5.2.4 Consideration (C) for the formula of wave-making resistance

In this Consideration (C), let us combine the results of the previous Considerations (A) and (B). Accordingly, by equating Eqs. (92) and (102), which are calculation formulae of the wave-making resistance R_W derived by various considerations in Sections 5.2.1 and 5.2.3, a highly meaningful relation can be achieved, as follows :

$$U\varepsilon^*\int_{-\infty}^{\infty}\frac{\partial\zeta}{\partial x}\cdot u_\Gamma\Big]_{z=0}dx-\frac{\kappa_0^* U^2}{4}\cdot Z_\zeta{}^2=0 \qquad \cdots\cdots(103)$$

Using the result above, R_W in Eqs. (92) and (102) can finally be expressed in the following simple form :

$$\frac{R_W}{\rho_A}=\frac{\kappa_0^* U^2}{4\varepsilon^*}\cdot Z_\zeta{}^2 \qquad \cdots\cdots(104)$$

According to the above formula, the wave-making resistance is explicitly determined as a quantity

corresponding to the square of the wave amplitude Z_ζ at the downstream, without cumbersome integral over an infinite interval. Here, if ε^* and κ_0^* defined in Eq. (16) are restored to the original ε and κ_0 and the definition of κ_0 in Eq. (4) are recalled, the wave-making resistance R_W can be expressed as follows :

$$R_W = \frac{1-\varepsilon}{4\varepsilon}\rho_A \kappa_0 U^2 Z_\zeta^2 = (1-\varepsilon)\cdot\left\{\frac{1}{4}\rho_W g Z_\zeta^2\right\} \quad \cdots\cdots(105)$$

In equation above, the value in the braces represents the wave-making resistance due to normal underwater disturbance without considering pressure fluctuations on the water surface. As a result, it can be seen that the wave-making resistance R_W, which takes into account pressure fluctuations due to aerial disturbance, is obtained as $(1-\varepsilon)$ times the value in the above braces.

When the density ratio ε is extremely small, as the case of air and water in Eq. (4), the error is at least quantitatively small, even if it is ignored and analyzed by the momentum theorem, as done by Bessho-Ishikawa. However, as the density ratio ε at the interface increases to some extent, it is understood that the correct wave-making resistance cannot be calculated without using Eq. (105), which was derived in the present paper.

Then, the dimensionless coefficient C_W of wave-making resistance, whose calculation results are showed in the next chapter, is defined by :

$$C_W = \frac{R_W}{\frac{1}{2}\rho_A U^2 c} \quad \cdots\cdots(106)$$

6. Examples of Numerical Calculation and Some Discussions

In this chapter, the results of numerical calculation, based on the theory developed up to the previous chapters, are presented. In the following, variables with $\tilde{()}$, such as $\tilde{x}, \tilde{z}, \tilde{h}, \tilde{\zeta}, \tilde{Z}_\zeta$, indicate dimensionless lengths with wing chord c as the criterion.

6.1 Element partitioning of wing and distribution density γ of vortex layer

Fig. 4 shows an example of element partitioning for the NACA23015 airfoil. In the figure, the face and back of the wing are divided into 40 elements each, for a total of 80 elements. However, all calculations in this chapter are performed by dividing minutely the wing surface into 160 elements, which is double the number of elements shown in this figure.

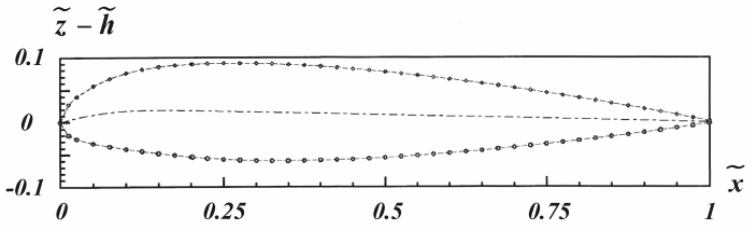

Fig. 4 Element partitioning of airfoil (NACA23015).

The flow field expression of Eq. (9) in Section 2.2 was discretized by the vortex layer model using 1st order elements in a segmented manner, and the calculation was performed as a thick airfoil. Details of this numerical method are described in Japanese paper by Hori [10]. However, the wavy term $\tilde{G}'_A$ of the Green's function in Eq. (18) were calculated by aggregating the vortex layers of each element into a vortex filament at the midpoint [9]. The numerical methods of computing the integral exponential function Ei in Eq. (32), which is necessary for the calculation of $\tilde{G}'_A$, are described in detail by Hori [9] in another paper. In this calculation, Taylor expansion in Eq. (33) is basically used, and in addition, continued fraction and asymptotic expansion are used in combination depending on the case.

Then, the unknown density γ of vortex layer is obtained by solving a boundary value problem with the Green's function G_A as the kernel function so as to satisfy the wing surface condition. In this case, we also need expressions for the derivative of G_A with respect to x and z. For more information on these, please refer to Hori's papers [8], [9].

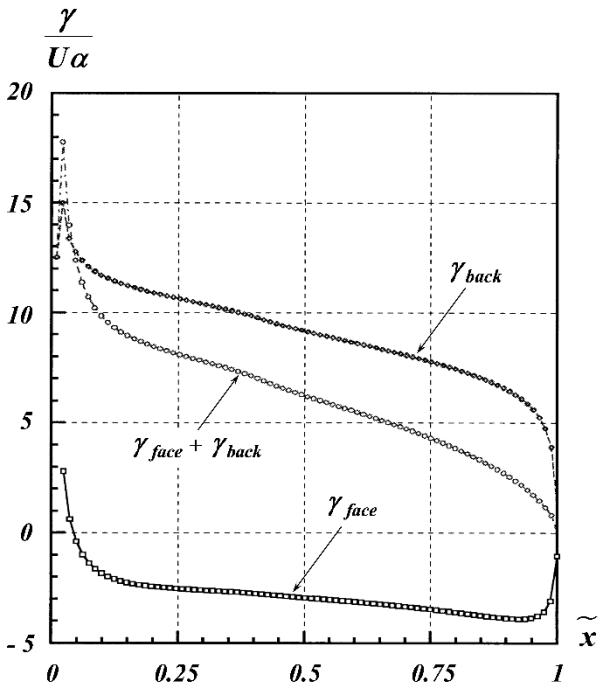

Fig. 5 Distribution density γ of the vortex layer of NACA4412 ($h = 0.1$, $\alpha = 8°$).

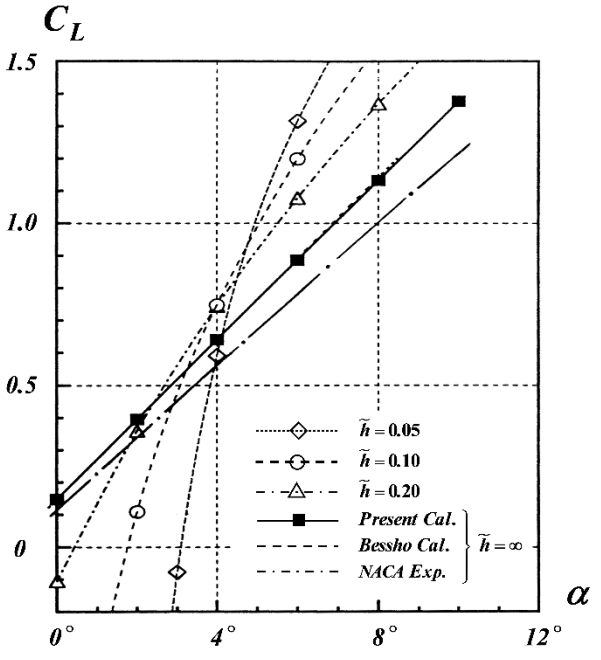

Fig. 6 Lift curve of NACA23015.

Fig.5 shows the distribution density $\frac{\gamma}{U\alpha}$ of the vortex layer, solved by the above method. The γ distributions indicate the face, back, and the sum of both surfaces, for a total of three curves. These are calculation results for NACA4412 airfoil using the so-called normal mirror image model, in which the water surface is replaced by a rigid wall. The calculation conditions of WIG are the angle of attack of $\alpha = 8°$ and the surfacing altitude of $h = 0.1$.

6.2 Lift force

First, Fig. 6 shows the lift curve of the NACA 23015 airfoil. C_L on the vertical axis is defined by Eq. (66). The result in the infinite fluid ($\tilde{h}=\infty$), shown by the solid line, almost overlaps with the Bessho-Ishikawa result[3] shown by the dashed line. It was confirmed that the numerical calculations using the vortex layer model were performed correctly. The difference from experimental results of NACA, shown by the single-dotted line, can be attributed to the fact that viscous effects were not taken into account in the calculations. Water surface effects were calculated using a normal mirror image model. From this result, it can be seen that at angles of attack higher than about $\alpha=4^\circ$, the lift increases and the surface effects are ensured as the surfacing altitude is lowered. On the other hand, at angles of attack lower than above, the lift decreases contrary as the altitude is lowered.

Next, Fig. 7 and Fig. 8 show the calculation of water surface effects of lift force for the NACA 23015 and NACA 4412 airfoils, respectively. Fig. 7 compares the present calculation with the Bessho-Ishikawa's result[4], and Fig. 8 compares it with the Kataoka-Ando-Nakatake's result[6].

The single-dotted line in both figures is the result for an infinite fluid ($\tilde{h}=\infty$). The solid lines with markers ● and ◆ are the calculation result for the flow field at high speed limits, which is represented by placing a slightly weaker vortex of $(1-2\varepsilon^*)\Gamma$ at the mirror image position in the water for an aerial vortex of strength Γ, as shown in Eq. (54) in Chapter 4. However, comparing this result with it of the normal mirror image model at low speed limits in Eq. (47) with the water surface as a rigid wall (equivalent to setting $\varepsilon^*=0$ in Eq. (54)), the difference between the two is not observed in both figures for the condition that the density ratio ε is considerably small as in the case of air and water in Eq. (4), and two are drawn overlapping each other.

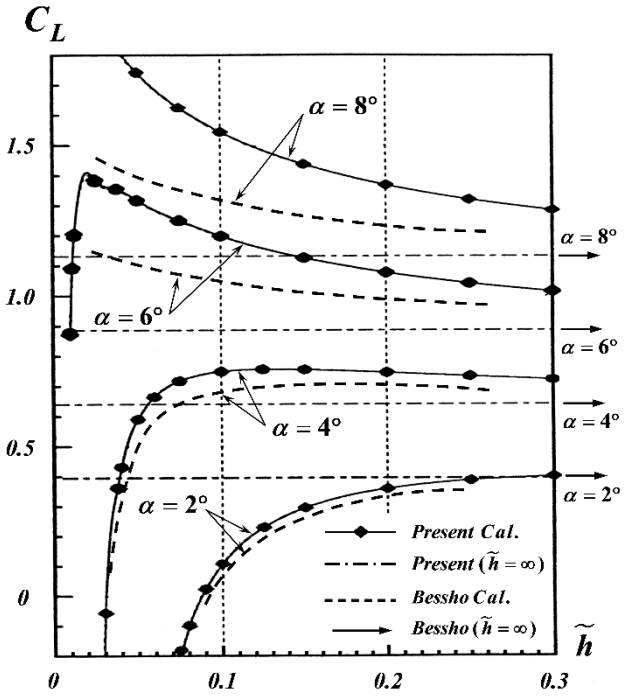

Fig. 7 Surface effects of lift acting on NACA23015.

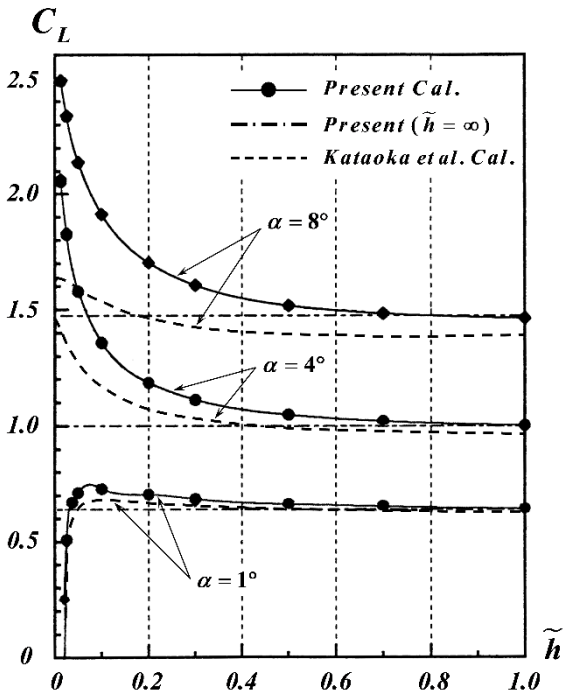

Fig. 8 Surface effects of lift acting on NACA4412.

The results in Fig. 7 show that the results of this paper and Bessho-Ishikawa, shown by right-pointing arrow →, are in very good agreement for $h=\infty$ regardless of the angle of attack α, as we found in Fig. 6.

As shown in Figs. 7 and 8, the calculation results in this paper, which take into account the water surface effects, are generally consistent with other results, Bessho-Ishikawa and Kataoka *et al.* shown by dashed line, up to $\alpha=4^\circ$. However, when the angle of attack increases to $\alpha=6^\circ, 8^\circ$, there is a tendency to calculate a larger lift force than the other results, especially when the surfacing altitude $\tilde{h}$ is low.

Considering the water surface effects, even for the same angle of attack of $\alpha=4^\circ$, the NACA23015 airfoil in Fig. 7 shows a decrease in lift as the surfacing altitude drops below $\tilde{h}=0.1$. In contrast, the NACA4412 airfoil in Fig. 8 seems to have the opposite tendency to increase lift. Accordingly, it can be seen that the lift characteristics due to water surface effects differ depending on the airfoil shape.

6.3 Water wave profile

Fig. 9 shows the wave profile $\tilde{\zeta}\ (=\zeta/c)$ generated by the NACA4412 airfoil for the four speed ranges $F_n=1,2,3,10$. The solid lines are calculated using the vortex distribution γ in Fig. 5 under the same conditions $\tilde{h}=0.1$, $\alpha=8^\circ$, by applying Eq. (39) in Chapter 3. Here, F_n on the horizontal axis is the Froude number, which is the dimensionless speed of the advanced velocity U normalized on the chord length c, and is defined as follows :

$$F_n=\frac{U}{\sqrt{g\,c}}=\frac{1}{\sqrt{\kappa_0 c}} \qquad \cdots\cdots(107)$$

The vertical axis in Fig. 9 shows that the wave height value itself is minute, and the deformation of

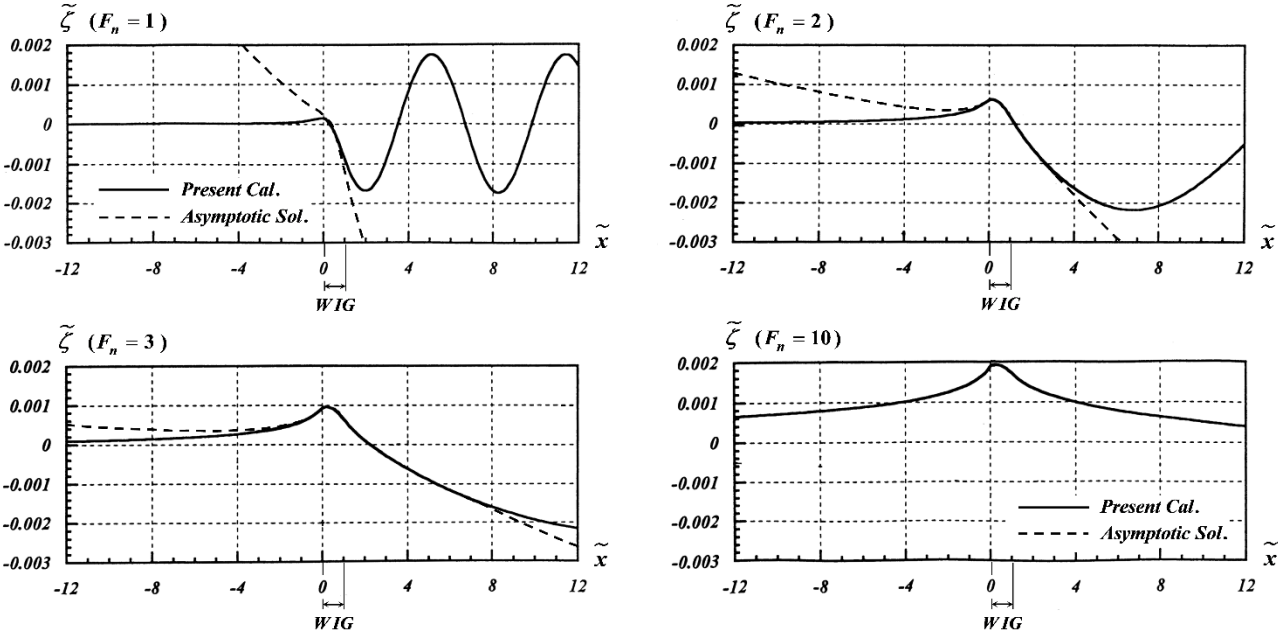

Fig. 9 Water wave profiles generated by NACA4412 ($h=0.1$, $\alpha=8^\circ$).

water surface caused by WIG is considerably small. It demonstrates that the validity of approximating the water surface as a rigid wall in the analysis.

The dashed lines are calculated by the high-speed asymptotic solution of the Green's function shown in Eq. (57) of Chapter 4, and provide a good approximation of the wave profile drawn by solid lines near the WIG, even at $F_n = 1, 2$. Furthermore, in the high speed range at $F_n = 3, 10$, it can be seen that the asymptotic wave profile is useful not only near the WIG, but also quite far away.

In any case, as predicted by the asymptotic solution in Eq. (57), it indicates that the wave surface rises in the neighborhood of WIG.

6.4 Wave-making resistance

Fig. 10 shows the results of examining the two types of wave-making resistance formulae proposed in Section 5.2 of present paper. C_W on the vertical axis is defined by Eq. (106). The calculations are performed for NACA0012 airfoil, with a surfacing altitude of $\tilde{h} = 0.01$ and an angle of attack $\alpha = 8^\circ$.

The solid line marked with □ is the coefficient of wave-making resistance C_W / ε^* of integrating on the still water surface over an infinite interval by using Eq. (92) in Consideration (A). In the present calculation, the entire integral interval on the still water surface $(-5 \le \tilde{x} \le 10)$ was divided into a total of 1580 segments. The numerical integral was performed in minute increments of $\delta\tilde{x} = 0.002$ near the trailing edge $(0.9 \le \tilde{x} \le 1.1)$ and in increments of $\delta\tilde{x} = 0.01$ for most of the rest.

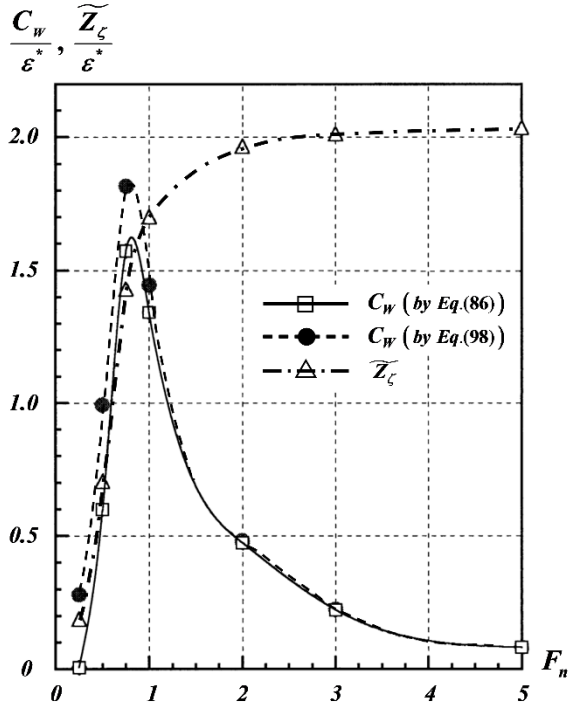

Fig. 10 Wave-making resistance and wave height acting on NACA0012 ($h = 0.01$, $\alpha = 8°$).

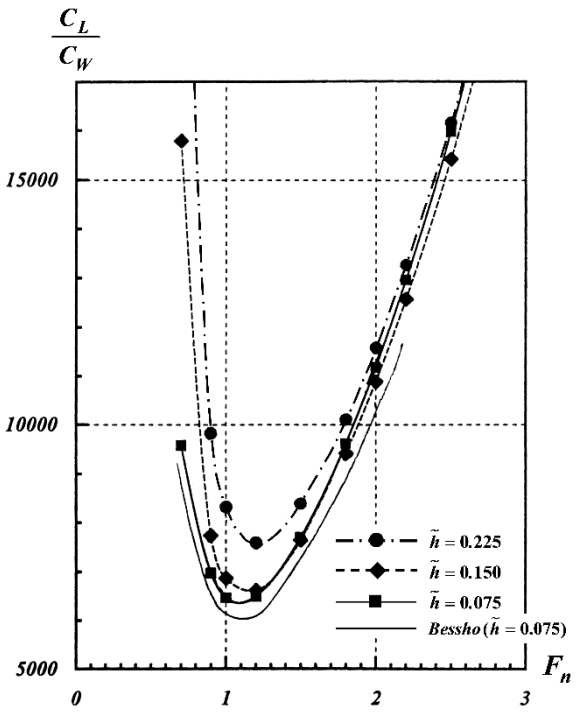

Fig. 11 Ratio of lift force to wave-making resistance acting on NACA23015 ($\alpha = 4°$).

On the other hand, the dashed line marked with ● is calculated by the square of the amplitude Z_ζ of the free wave in the downstream, as shown in the following simple formula, which is a rewrite of Eq. (104) in Consideration (C) by definition of Eqs. (106) and (107).

$$\frac{C_W}{\varepsilon^*} = \frac{1}{2}\left(\frac{\tilde{Z}_\zeta}{\varepsilon^* F_n}\right)^2 \quad \cdots\cdots(108)$$

Here, the above $\tilde{Z}_\zeta$ $\left(= Z_\zeta / c\right)$ is drawn in the same figure by a single-dotted line marked with △.

As a result, it can be seen that the two curves marked by □ and ● are in good agreement, even though they were obtained using different calculation formulae. For both curves, the values C_W / ε^* peak at around $F_n = 0.8$. This confirmed numerically that the wave-making resistance value of the WIG can be calculated using Eq. (104) without the troublesome integral over the water surface as in Eq. (92). However, at speeds slower than $F_n = 1$, the value of ● obtained by $\tilde{Z}_\zeta^{\,2}$ is slightly larger than that of □. This may also be related to the length of entire integral interval and numerical increments on the still water surface mentioned above, so the reason should be further investigated.

Fig. 11 shows the lift-to-drag ratio C_L / C_W of the aerodynamic forces acting on a NACA23015 airfoil with an angle of attack $\alpha = 4^\circ$ and surfacing altitudes $\tilde{h} = 0.075, 0.150, 0.225$, and is organized based on F_n. The lift force C_L in the numerator is shown in Fig. 7, and the drag C_W in the denominator is the wave-making resistance. In this case, the ratio takes its minimum value at around $F_n = 1.2$. This is because the lift force C_L in the numerator remains nearly constant under above conditions of α and $\tilde{h}$ as shown in Fig. 7, while the wave-making resistance C_W in the denominator reaches its peak value at this point. Then, regardless of the Froude number F_n on the horizontal axis, this ratio increases slightly as the surfacing altitude rises. This is also thought to be because the wave-making phenomena wane as the surfacing altitude $\tilde{h}$ from the water surface rises, resulting in a smaller wave-making resistance value C_W in the denominator.

In addition, at low altitude of $\tilde{h} = 0.075$, the ratio C_L / C_W in present paper, marked by ■, is shown in good qualitative and quantitative agreement with the Bessho-Ishikawa calculation, drawn by the unmarked solid line. Accordingly, the validity of the calculations in this paper for the wave-making resistance value C_W of the WIG was also confirmed.

7. Concluding Remarks

The water surface effects of WIG were analyzed for a 2-dimensional problem in which pressure fluctuations on the water surface due to aerial disturbance were correctly considered. And a new form of Green's function considering water wave generation caused by aerial vortices was derived by Fourier transform method, taking into account the effect of water surface deformation on the aerial side, which has been neglected in the past.

By examining an asymptotic form of the Green's function, it is shown that the high-speed flow field due to an aerial vortex of strength Γ can be represented by placing a slightly weaker vortex of

$(1-2\frac{\varepsilon}{1+\varepsilon})\Gamma$ (where, $\varepsilon = \frac{\rho_A\ (density\ of\ Air)}{\rho_W\ (density\ of\ Water)}$) at the mirror image position under the water surface. Then, an asymptotic solution of water wave profile was proposed. In the high speed range, the wave height near the clockwise aerial vortex, corresponding to WIG, is obtained positively, indicating that the wave surface is raised.

The lift force and wave-making resistance acting on the WIG were analyzed based on the momentum theorem, and smart calculation formulae were derived for two forces, resulting that the following two things were found. The lift force can be calculated by the well-known Kutta-Joukowski's theorem as well, which holds in the case of an ordinary wing. Regarding the wave-making resistance, an explicit formula, by which the resistance can be calculated in proportional to simply the square of the amplitude Z_ζ of trailing free waves at downstream without the need for tedious integral over the still water surface, is derived by detailed considerations. And the resistance value is computed as $(1-\varepsilon)$ times the value, obtained by the conventional calculation formula for the underwater disturbance.

Based on the fundamental theory developed in present paper, specific numerical calculations of aerodynamic forces and water wave profile were also performed for thick wings such as NACA airfoils, and comparisons ware made with other calculation examples. As a result of the examination, the validity of present theory was confirmed and a certain amount of knowledge was gained regarding the water surface effects of WIG.

As described above, a method for calculating water surface effects on the aerodynamic characteristics of a 2-dimensional WIG has been proposed by constructing the new form of wave-making Green's function. Future research requires some systematic numerical calculations for various conditions and an extension of the theory to 3-dimensional problems.

Acknowledgments

A part of this study was conducted with the support of a Grants-in-Aid for Scientific Research from *the Ministry of Education, Culture, Sports, Science and Technology - Japan*, as one of the collaborating researcher. The contents of this grant are that *Grant Number* : ***08305039***, *Grant Category* : Fundamental Research (B), *Research Subject* : Study on Performance Evaluation Methods for Wings attached to Ship utilizing Sea-Surface Effects, *Principal Researcher* : *Prof. Kiyoshige MATSUMURA*, Faculty of Engineering, *Osaka University*, Japan. In closing this paper, we would like to note hereby and express our gratitude to principal researcher and all parties involved.

Finally, let me thank my daughter, *Manami* (White Swiss Shepherd Dog of 7 years old, her certified pedigree's name is *Jewel Manami HORI of Five Stars JP*). The reason is why she is always watching over me while I write a treatise at home and promptly translates my Japanese text into English.

In addition, the numerical computations in Chapter 6 were performed using absoft C/C++, which is C-language compiler installed in Power Macintosh 8500/120 on our laboratory desk.

References †

(1) Hori, T. : "Aerodynamic Characteristics of WIG by Proposal of New Green Function Considering Water Wave Generation Caused by Vortex System in the Air" (in Japanese), ***NAVIGATION*** (*Transactions of Japan Institute of Navigation*), 2015 (January), ***No.191***, pp. 77~86, This reference is the basis for present paper.

(2) Tomotika, S. and Imai, I. : " The Interference Effect of the Surface of the Sea on the Lift of Seaplane " (in English), *Report of Aeronautical Research Institute, Tokyo Imperial University,* 1937 (February), ***Vol.12 : No.146***, pp. 69~128.

(3) Tani, I. : " The Effect of Ground upon the Aerodynamic Characteristics of a Wing " (in Japanese), The *Journal of the Society of Aeronautical Science of Nippon,* 1937 (June), ***Vol.4 : No.26***, pp. 659~674.

(4) Bessho, M. and Ishikawa, A. : " On the Water Surface Effect of an Air Wing (1st Report)" (in Japanese), *Journal of the Kansai Society of Naval Architects, Japan,* 1977 (June), ***No.165***, pp. 59~69.

(5) Masuda, S. and Suzuki, K. : "Simulation of Hydrodynamic Effects of 2-Dimensional WIG Moving near the Free Surface" (in Japanese), *Journal of the Society of Naval Architects of Japan,* 1991 (December), ***Vol.170***, pp. 83~92.

(6) Kataoka, K., Ando. J. and Nakatake, K. : "Free Surface Effect on Characteristics of Two-Dimensional Wing" (in Japanese), *Transactions of the West-Japan Society of Naval Architects*, 1992 (March), ***No.83***, pp. 21~30.

(7) Hori, T. : "Proposal of New Green Function Considering Wave Generation Caused by Vortex System in the Air —No.1 Linearized Theory in 2-D WIG—" (in Japanese), *Bulletin of Institute for Innovative Science and Technology, Nagasaki Institute of Applied Science,* 2007 (March), ***No.2***, pp. 89~95.

(8) Hori, T. : "A Numerical Analysis of the Neumann-Kelvin Problem on Steady Wave Generation —(1st Report) Some Numerical Discussions for a Two-Dimensional Submerged Circular Cylinder—" (in Japanese), *Bulletin of Nagasaki Institute of Applied Science*, 1992 (October), ***No.33*** (50th Anniversary Commemorative Issue), pp. 161~184.

(9) Hori, T. : " Simulation Study of Water Wave Generation Caused by Running 2-D Hydrofoil " (in Japanese), ***NAVIGATION*** (*Transactions of Japan Institute of Navigation*), 2016 (April), ***No.196***, pp. 99~108.

(10) Hori, T. : "Analysis on the Aerodynamic Characteristics of Thick Wings using the Vortex Layer Model with 1st Order Elements —Recommendations for Scientific and Technical Computing on Macintosh—" (in Japanese), *Bulletin of Computer Science Center, Nagasaki Institute of Applied Science*, 1997 (March), ***No.7 : 1996***, pp. 40~48.

† Bold text in the list means that there is a HyperLink.

長崎総合科学大学紀要 ONLINE ISSN 2423-9976 / 65巻 / 2号

発行日 2026-01-15 1 - 2 of 2 results.

AI（人工知能）による振動水柱型波力発電装置の効率向上に関する研究

AI（人工知能）による振動水柱型波力発電装置の効率向上に関する研究

影本, 浩, 藤島, 研一, 中村, 爽太郎 p. 27-48 pdf

Analysis on Aerodynamic Characteristics of WIG
— Proposal of New Green's Function
considering Water Wave Generation caused by Aerial Vortices —

Analysis on Aerodynamic Characteristics of WIG
— Proposal of New Green's Function
considering Water Wave Generation caused by Aerial Vortices —

Hori, Tsutomu p. 49-78 pdf